

Novel quantum phases on graphs using abelian gauge theory

Pramod Padmanabhan,^a Fumihiko Sugino^b

^a*School of Basic Sciences,
Indian Institute of Technology, Bhubaneswar, India*

^b*Center for Theoretical Physics of the Universe,
Institute for Basic Science, Daejeon, South Korea*

pramod23phys, fusugino@gmail.com

Abstract

Graphs are topological spaces that include broader objects than discretized manifolds, making them interesting playgrounds for the study of quantum phases not realized by symmetry breaking. In particular they are known to support anyons of an even richer variety than the two-dimensional space. We explore this possibility by building a class of frustration-free and gapped Hamiltonians based on discrete abelian gauge groups. The resulting models have a ground state degeneracy that can be either a topological invariant, an extensive quantity or a mixture of the two. For two basis of the degenerate ground states which are complementary in quantum theory, the entanglement entropy is exactly computed. The result for one basis has a constant global term, known as the topological entanglement entropy, implying long-range entanglement. On the other hand, the topological entanglement entropy vanishes in the result for the other basis. Comparisons are made with similar occurrences in the toric code. We analyze excitations and identify anyon-like excitations that account for the topological entanglement entropy. An analogy between the ground states of this system and the θ -vacuum for a $U(1)$ gauge theory on a circle is also drawn.

Contents

1	Introduction	2
2	The operators	4
2.1	Vertex operator or gauge transformations	5
2.2	Edge operators or 0-holonomy operators	6
2.3	The Hamiltonian	7
3	Ground states	9
3.1	GSD	10
3.2	Construction of ground states	11
3.3	Ground states $ \text{GS}[\alpha, \beta]\rangle$	15
4	Entanglement Entropy	19
4.1	Bipartite EE for $ \text{GS } s\rangle$	20
4.2	Bipartite EE for $\rho^{[\alpha, \beta]}$	24
5	Excited states	28
5.1	Edge excitations	29
5.2	Vertex excitations	30
5.3	Case of $m = 4, n = 6$	32
5.4	Anyon-like excitations and topological EE	34
5.5	Exchange statistics on graphs	36
6	Discussion	39
6.1	Summary	39
6.2	Outlook	40
A	Analogy to quantum field theory with $U(1)$ gauge field and a matter field	43

B	$U(1)$ gauge theory on a circle	43
C	Short review of graph homology	45

1 Introduction

Quantum phases of matter, or the ones that are beyond Landau’s classification of spontaneous symmetry breaking with local order parameters, have gained theoretical and experimental significance over the last few decades. Among them, the so called *topological phases of matter* or the *topologically ordered* phases have become increasingly important for robust methods of quantum computation [1–3]. While topological order can manifest itself in different ways in different dimensions, a class of solvable examples in two dimensions are given by the quantum double models of Kitaev [4]. They are characterized by a ground state degeneracy (GSD) that is a topological invariant, anyonic excitations, and ground state entanglement entropy (EE) that includes a global component depending on the superselection sectors of the theory [5] as a subleading order term. The quantum double models are Hamiltonian realizations of discrete gauge theories or gauge theories based on finite groups which were well studied in the early 90’s [6]. More generally they can also be considered for *involutory Hopf algebras* [7], of which the group algebra is a special case [4, 8, 9].

Most studies consider long-ranged topologically ordered systems in two and three dimensions. The models predominantly are located on lattices that discretize a two- or three-dimensional differentiable manifold. In this paper we construct exactly solvable models for quantum phases on *connected graphs* which do not fall into the usual setups for physical systems, since graphs include broader objects than discretized manifolds. However a graph is still a *topological space* and can be conveniently thought of as a one-dimensional CW complex [10]. In fact physics on graphs or networks, as it is sometimes called in the literature, can be rather non-trivial, with early works studying the issue of particle statistics on such spaces [11].¹ More importantly, there have been studies exploring the possibilities of anyons on graphs, both abelian and non-abelian ones [15–18]. Analogous to *braid groups* being the fundamental groups of the configuration space of N identical particles in \mathbb{R}^2 [19], *graph braid groups* play a similar role on different types of graphs [20–22]. However, these have a fundamental differ-

¹Graph structures also appear in the physics and math literature under the name of *quantum graphs* especially in the area of mesoscopic physics [12–14].

ence from the conventional braid groups, as the generators do not obey a Yang-Baxter type relation.

It is reasonable to expect that our models on graphs share some features with systems of the known topologically ordered phases. The goal of this paper is to explore this possibility by analyzing models based on discrete abelian gauge groups, which are quite similar in form to the abelian quantum double models or the toric code. The main difference is that now we also include ‘matter’ fields on the vertices of the lattice or graph in addition to the gauge fields on the edges/links of the lattice or graph. While the vertex operators or the gauge transformations of the toric code are slightly modified to act on the matter fields on the vertices as well, the plaquette operators or the operators measuring local flux of the toric code are replaced by an entirely new operator known as the *edge operator*. Before we go into the details of the models we would like to emphasize that the models presented here can be obtained from [23–27] where topological order is discussed from the point of view of *higher gauge theories* [28] constructed using 2-groups and other higher categories. The papers [23,24] study topological order in various dimensions using simplicial complexes and in this context what we present here is a detailed study of the models in the simplest such complex, namely a graph.

The rest of this paper is organized as follows. The operators on graphs, including the Hamiltonian, are defined in section 2. The models are parametrized by two integers, m and n , which are the dimensions of the local Hilbert spaces on the vertices and edges of the graph, respectively. Following this we cover all the tell-tale signs of topological order starting with a detailed analysis of the ground states in section 3. For general m and n , we find the GSD to be a function of a topological invariant (the first Betti number) and a graph invariant (the number of vertices). The latter gives an extensive dependence on the system size.² Next we exactly compute the EE of these ground states in section 4, and find that there is a global constant term known as the topological EE, which exists regardless of the partition of the graph. We also compute the EE for superpositions of the ground states that are complementary to the previous ground states, in which the topological EE turns out to vanish. Different aspects from arguments on the *minimal entropy states* given in [30,31] are observed here. In section 5 we see that the total quantum dimension of the system obtained from the topological EE is precisely equal to the number of anyon-like excitations. In section 6 we summarize the result

²Graph invariants are invariant quantities under graph isomorphisms. There are more non-trivial graph invariants known as *Tutte polynomials* which also arise in statistical physics [29].

and discuss some future directions. In appendix A, we present an analogy of the model to quantum field theory with $U(1)$ gauge field and matter field to gain an intuitive understanding. In appendix B, $U(1)$ gauge theory on a circle obeying twisted boundary conditions is briefly discussed to help understand the ground states of our models. Appendix C is devoted to some topological aspects of graphs.

2 The operators

Let $G = (V, E)$ be a connected graph composed by a set of vertices V and a set of edges E . Each edge is endowed with an orientation and its endpoints are attached to vertices in V . For each of such graphs, the adjacency matrix is well-defined.³

We place finite dimensional Hilbert spaces on both the vertices and the edges making the total Hilbert space, $\mathcal{H} = \otimes_{v \in V} \mathcal{H}_v \otimes_{e \in E} \mathcal{H}_e$. Upon taking $\mathcal{H}_v = \text{Span of } \{|h_v\rangle | h_v = 0, 1, \dots, m-1\} \simeq \mathbb{C}^m$ for each v and $\mathcal{H}_e = \text{Span of } \{|i_e\rangle | i_e = 0, 1, \dots, n-1\} \simeq \mathbb{C}^n$ for each e , we can consider the local Hilbert spaces as carrying the representations of the abelian groups, \mathbb{Z}_m and \mathbb{Z}_n respectively. In the parlance of many-body physics these are m and n level systems or spins $\frac{m-1}{2}$ and $\frac{n-1}{2}$ on the vertices and edges respectively.

Furthermore we consider a homomorphism, $\partial : \mathbb{Z}_n \rightarrow \mathbb{Z}_m$. For any \mathbb{Z}_n elements $a, b \in \{0, 1, \dots, n-1\}$, the homomorphism satisfies $\partial(a+b) = \partial(a) + \partial(b)$. The \mathbb{Z}_n degrees of freedom on each edge are regarded as ‘gauge fields’, and the \mathbb{Z}_m degrees of freedoms on each vertex as ‘matter fields’. The homomorphism induces the gauge transformation property of the matter fields from that of the gauge fields. Let k be the greatest common divisor of m and n ($\text{gcd}(m, n) = k$). Then, we can write m and n as

$$m = kp, \quad n = kq, \quad (2.1)$$

where p and q are coprime integers ($\text{gcd}(p, q) = 1$). The possible choices for the homomorphism are labelled by the group \mathbb{Z}_k and given by

$$\partial^{[l]}(j) = pj \quad (2.2)$$

with $l \in \mathbb{Z}_k = \{0, 1, \dots, k-1\}$ labelling the homomorphisms. These give compatible homomorphisms as $\partial^{[l]}(n) = pnl = m$, under mod m arithmetic, implying that $\partial^{[l]}$ ’s map the

³The (i, j) -th matrix element stands for the number of edges directed from the i -th vertex to the j -th vertex. The diagonal (i, i) -th matrix element counts the number of self-loops at the i -th vertex.

identity of \mathbb{Z}_n to the identity of \mathbb{Z}_m . For later convenience, we also introduce the greatest common divisor of k and p which is denoted by ξ : $\gcd(k, p) = \xi$. Namely,

$$k = \xi \tilde{k}, \quad p = \xi \tilde{p} \quad \text{with} \quad \gcd(\tilde{k}, \tilde{p}) = 1. \quad (2.3)$$

Using these ingredients we define the operators that make up the Hamiltonian. Although it is possible for a general l , the case $l = 1$ is mainly considered in what follows for simplicity. Then (2.2) becomes $\partial(j) = pj$.

2.1 Vertex operator or gauge transformations

The *vertex operator*, A_v , implements the gauge transformations of the gauge group \mathbb{Z}_n , and acts nontrivially on \mathcal{H}_v and \mathcal{H}_e with the edges e attached to v . Let L_v be the set of edges attached to the vertex v . L_v is divided into a set of edges directed inwards to v , L_v^+ , and a set of edges directed outwards from v , L_v^- : $L_v = L_v^+ \cup L_v^-$. For the example depicted in Fig. 1, $L_v^+ = \{e_1, \dots, e_r\}$ and $L_v^- = \{e_{r+1}, \dots, e_{r+s}\}$.

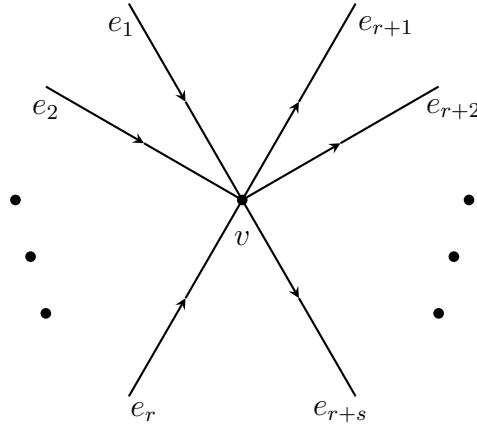


Figure 1: A vertex v and attached $r + s$ edges. The left r edges (e_1, e_2, \dots, e_r) are directed to the vertex, whereas the right s edges ($e_{r+1}, e_{r+2}, \dots, e_{r+s}$) are outgoing from the vertex.

The operator A_v is defined as

$$A_v = \frac{1}{n} \sum_{j=0}^{n-1} A_v^{(j)}, \quad A_v^{(j)} \equiv x_v^{\partial(j)} \mathbf{X}_{L_v}^{pj} \quad (2.4)$$

with

$$\mathbf{X}_{L_v} \equiv \left(\prod_{e \in L_v^+} X_e \right) \left(\prod_{e \in L_v^-} X_e^{-1} \right). \quad (2.5)$$

x_v and X_e are the shift operators on the basis of \mathbb{C}^m and \mathbb{C}^n respectively:

$$x_v |h_v\rangle = |h_v + 1\rangle, \quad X_e |i_e\rangle = |i_e + 1\rangle, \quad (2.6)$$

where the numbers h_v and i_e are evaluated in mod m and mod n arithmetic respectively. For the example in Fig. 1, $A_v^{(j)} = x_v^{\partial(j)} \left(\prod_{a=1}^r X_{e_a}^{pj} \right) \left(\prod_{b=r+1}^{r+s} X_{e_b}^{-pj} \right)$ acts on the local Hilbert spaces as

$$A_v^{(j)} \left(|h_v\rangle \prod_{a=1}^r |i_{e_a}\rangle \prod_{b=r+1}^{r+s} |i_{e_b}\rangle \right) = |h_v + pj\rangle \prod_{a=1}^r |i_{e_a} + pj\rangle \prod_{b=r+1}^{r+s} |i_{e_b} - pj\rangle. \quad (2.7)$$

The vertex operator (2.4) is easily seen to be a projector $(A_v)^2 = A_v$, as it is a *group average* over \mathbb{Z}_n . It has $n - 1$ other mutually orthogonal projectors⁴ that are labelled by the *irreducible* representations (IRRs) of \mathbb{Z}_n ,

$$A_v^{[\alpha]} = \frac{1}{n} \sum_{j=0}^{n-1} \chi_{\alpha,n}(j) A_v^{(j)}, \quad (2.8)$$

where α labels the IRR and $\chi_{\alpha,n}(j)$ is the character of the element $j \in \mathbb{Z}_n$ in the IRR α . Explicitly, $\chi_{\alpha,n}(j) = \omega_n^{\alpha j}$ with $\alpha \in \{0, 1, \dots, n-1\}$. Here and in what follows, $\omega_d \equiv e^{\frac{2\pi i}{d}}$ for a positive integer d . In this notation the vertex operator in (2.4) corresponds to the trivial IRR ($\alpha = 0$).

2.2 Edge operators or 0-holonomy operators

The plaquette operators in the toric code or more generally the quantum double models [4] measure the flux of the gauge fields around a plaquette (or in other words the smallest *Wilson loop*) for the discrete gauge group. We call this the *1-holonomy* operator.⁵ In a similar manner, we consider the ‘0-holonomy’ operator or edge operator which acts on two adjacent vertices and the link in-between as in Fig. 2.

⁴These properties follow from the *orthogonality theorem* for group characters, also known as the *Schur orthogonality relations* [32].

⁵We use 0-holonomy and 1-holonomy keeping in mind that these operators can be generalized to abelian *higher gauge groups* as in [23]. In the language of higher gauge theory as described in [23], matter fields on vertices are 0-gauge fields and the gauge fields on edges are 1-gauge fields. This can be generalized to d -gauge fields living on d -dimensional simplices of a simplicial complex.

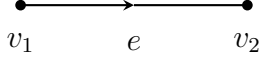


Figure 2: A directed edge e flanked by vertices v_1 and v_2 .

It is defined as⁶

$$B_e = \frac{1}{k} \sum_{j=0}^{k-1} B_e^{(j)} \quad \text{with} \quad B_e^{(j)} \equiv z_{v_1}^{pj} Z_e^{qj} z_{v_2}^{-pj}, \quad (2.9)$$

where z_v and Z_e are clock operators on the basis of \mathbb{C}^m and \mathbb{C}^n respectively:

$$z_v |h_v\rangle = \omega_m^{h_v} |h_v\rangle, \quad Z_e |i_e\rangle = \omega_n^{i_e} |i_e\rangle. \quad (2.10)$$

It is easy to see that B_e is a projector $(B_e)^2 = B_e$ and is diagonal on the basis. It turns out that the edge operator or 0-holonomy operator (2.9) acts on the local Hilbert spaces as

$$B_e |h_{v_1}\rangle |h_{v_2}\rangle |i_e\rangle = \delta_m(p(h_{v_2} - h_{v_1}), \partial(i_e)) |h_{v_1}\rangle |h_{v_2}\rangle |i_e\rangle \quad (2.11)$$

with $\delta_m(a, b)$ being the mod m Kronecker delta for integers a and b . Physically this can be regarded as measuring the 0-flux due to the matter fields or the 0-gauge fields across the 1-gauge field on the edge e .

As with the vertex operators, we can write down the orthogonal projectors of these edge operators by projecting to different IRRs of \mathbb{Z}_m as

$$B_e^{[\alpha]} = \frac{1}{k} \sum_{j=0}^{k-1} \chi_{\alpha, m}(pj) B_e^{(j)}. \quad (2.12)$$

Since $\chi_{\alpha, m}(pj) \equiv \omega_m^{\alpha pj} = \omega_k^{\alpha j}$, independent operators are given by $\alpha \in \mathbb{Z}_k = \{0, 1, \dots, k-1\}$ rather than \mathbb{Z}_m .

2.3 The Hamiltonian

For a graph $G = (E, V)$, the Hamiltonian H is constructed out of the vertex and edge operators (2.4) and (2.9) as⁷

$$H = - \sum_{v \in V} A_v - \sum_{e \in E} B_e. \quad (2.13)$$

⁶Due to the presence of the gauge field on e this operator is sometimes called as the ‘fake’ 0-holonomy in the literature [23, 24, 26, 27]. Also, when the vertices v_1 and v_2 coincide ($v_1 = v_2 \equiv v$) and the edge e forms a self-loop, $B_e^{(j)}$ becomes $B_e^{(j)} = 1_v Z_e^{qj}$ with 1_v the identity operator on \mathcal{H}_v .

⁷For a general choice of the homomorphism l , the vertex operator (2.4) with $\partial(j)$ replaced by $\partial^{[l]}(j)$ and the edge operator (2.9) with Z_e^{qj} changed by Z_e^{qjl} , compose the Hamiltonian.

From the properties of the shift and clock operators

$$x_v^{j_1} z_v^{j_2} = \omega_m^{-j_1 j_2} z_v^{j_2} x_v^{j_1} \quad \text{and} \quad X_e^{j_1} Z_e^{j_2} = \omega_n^{-j_1 j_2} Z_e^{j_2} X_e^{j_1}, \quad (2.14)$$

it is easy to show that projectors A_v and B_e mutually commute with each other:

$$[A_v, B_e] = [A_v, A_{v'}] = [B_e, B_{e'}] = 0 \quad (2.15)$$

for any $v, v' \in V$ and $e, e' \in E$.⁸ The operators A_v and B_e either have no overlap or share one edge and one vertex. In the latter case, noncommutativity of the operators on the edge cancels with that of the operators at the vertex, which is analogous to the abelian toric code models [4]. Thus the Hamiltonian (2.13) is a sum of commuting projectors, and hence it is gapped and frustration-free.

Note that the operators in the Hamiltonian are well-defined for an arbitrary graph irrespective of it being planar or non-planar. Although we only consider the case where the gauge group is \mathbb{Z}_n and the matter fields belong to \mathbb{Z}_m , the model can be extended to an arbitrary abelian group. An analogy to quantum field theory with $U(1)$ gauge field and a matter field is presented in appendix A.

We mention some symmetry properties of the system:

- **Local symmetries** - It is easy to verify that $x_v \mathbf{X}_{L_v}$ and X_e^k for any $v \in V$ and $e \in E$ commute with the Hamiltonian (2.13), and generate local $\mathbb{Z}_{k p q}$ and \mathbb{Z}_q symmetries respectively. z_v^k and $Z_e^{\tilde{n}}$ with

$$\tilde{n} \equiv \frac{n}{\xi} = \tilde{k} q \quad (2.16)$$

are also local operators commuting with the Hamiltonian (ξ is the greatest common divisor of k and p as in (2.3)).

Seemingly x_v^k for any $v \in V$ is an additional local \mathbb{Z}_p symmetry transformation, but it is equivalent to one of the above transformations: $(x_v \mathbf{X}_{L_v})^{k q} = x_v^{k q}$ due to $\gcd(p, q) = 1$.

- **Quasi-local symmetries** - Consider traversing a closed path C , consisting of edges in E , in either the clockwise or counterclockwise direction. Then we can write down the operator

$$Z(C) \equiv \prod_{e \in C} Z_e^{(e|C)}, \quad (2.17)$$

⁸This can also be seen from the actions on the local Hilbert spaces (2.8) and (2.11), which can be used for generalizations to arbitrary finite non-abelian groups as well [25].

where $(e|C)$ is a sign factor according the orientations: $(e|C) = 1$ for e and C parallel, and $(e|C) = -1$ for e and C anti-parallel. This operator is analogous to the Wilson loop of the gauge theory, and commutes with the Hamiltonian (2.13). The number of such independent operators is equal to the number of independent closed paths on the graph: $|E| - |V| + 1$, where $|E|$ and $|V|$ are the numbers of edges and vertices in the graph. This is equal to the *first Betti number*, a topological invariant of the graph.⁹ For planar graphs, the first Betti number can be interpreted as the number of one-dimensional holes.

- **Global symmetries** - The operator, $\prod_{v \in V} x_v$, with support spanning all the vertices of the graph commutes with the Hamiltonian (2.13) and generates a global \mathbb{Z}_m symmetry. This is deduced from the above local symmetry as $\prod_{v \in V} x_v \mathbf{X}_{L_v}$ upon using the constraint $\prod_{v \in V} \mathbf{X}_{L_v} = 1$. The Hamiltonian is also invariant under parity, which is realized on a directed graph by reversing the orientations of all the edges, seen via taking the inverse of the shift and clock operators on all vertices and edges.

Notice that the local transformation X_e^k does not commute with the quasi-local transformation (2.17) when e is on the path C . Thus, any state cannot respect both of the two symmetries. Similarly, $x_v \mathbf{X}_{L_v}$ does not commute with z_v^k and $Z_e^{\tilde{n}}$.

3 Ground states

The Hamiltonian (2.13) is exactly solvable. Since the $\text{Spec}(A_v) = \text{Spec}(B_e) = \{0, 1\}$ for all v and e , the lowest energy is given by $E_0 = -|V| - |E|$, and any ground state $|\text{GS}\rangle$ satisfies $A_v|\text{GS}\rangle = B_e|\text{GS}\rangle = |\text{GS}\rangle$ for all $v \in V$ and $e \in E$. From this it follows that the projector to the ground state manifold is given by

$$\pi_0 = \prod_{v \in V} A_v \prod_{e \in E} B_e. \quad (3.1)$$

It is clear then that the GSD is given by the trace of π_0 over the total Hilbert space:

$$\text{GSD} = \text{Tr}_{\mathcal{H}} (\pi_0). \quad (3.2)$$

⁹Topological aspects of the first Betti number are provided with a brief look at graph homology theory in appendix C.

3.1 GSD

To compute the trace we observe that the non-zero contribution comes from the term $\prod_{v \in V} 1_v \prod_{e \in E} 1_e$ in π_0 , where 1_v and 1_e are the identity operators on \mathcal{H}_v and \mathcal{H}_e respectively. Note that $\text{Tr}_{\mathcal{H}} = \left(\prod_{v \in V} \text{Tr}_v \right) \left(\prod_{e \in E} \text{Tr}_e \right)$ with Tr_v and Tr_e being the traces over the Hilbert spaces \mathcal{H}_v and \mathcal{H}_e . For the shift and clock operators, $x_v^m = z_v^m = 1_v$ and $x_v^a z_v^b$ is traceless unless $a, b \in m\mathbb{Z}$. The same holds for X_e and Z_e . Then, from (2.4), (2.9) and (3.1), π_0 is written as a polynomial of x_v, z_v, X_e and Z_e for all $v \in V, e \in E$. Among the terms of the polynomial, only the term proportional to the identity $\prod_{v \in V} 1_v \prod_{e \in E} 1_e$ gives non-zero contribution under the trace operation in (3.2). Any other term contains at least one of x_v, z_v, X_e and Z_e for some $v \in V, e \in E$, and vanishes under the trace.

Thus computing the GSD translates into an exercise of counting the number of $\prod_{v \in V} 1_v \prod_{e \in E} 1_e$'s in π_0 . The answer should be the multiplication of the three factors:

- $\left(\frac{1}{n}\right)^{|V|} \left(\frac{1}{k}\right)^{|E|}$ from the prefactors of the sums in A_v (2.4) and B_e (2.9)
- the dimension of the total Hilbert space $m^{|V|} n^{|E|}$
- the number of $\prod_{v \in V} 1_v \prod_{e \in E} 1_e$'s.

When $j = k, 2k, \dots, (q-1)k$ the operator x_v^{pj} in $A_v^{(j)}$ (2.4) becomes the identity, but the operators on the edges in $A_v^{(j)}$ remain nontrivial. Note that $pj/k \neq 0 \pmod{q}$ because of $\text{gcd}(p, q) = 1$. Also, for $j = 1, 2, \dots, k-1$, Z_e^{qj} in $B_e^{(j)}$ (2.9) is always nontrivial, which physically implies that there is no matter field with neutral electric charge. These properties lead to¹⁰

$$\begin{aligned} \text{GSD} &= \text{Tr}_{\mathcal{H}} \left(\prod_{v \in V} A_v \prod_{e \in E} B_e \right) \\ &= \left(\frac{1}{n}\right)^{|V|} \left(\frac{1}{k}\right)^{|E|} \times m^{|V|} n^{|E|} \times q \\ &= p^{|V|} q^{B_1}, \end{aligned} \tag{3.3}$$

where $B_1 = |E| - |V| + 1$ is the first Betti number of the graph. For any fixed $j \in k\mathbb{Z}_q = \{0, k, 2k, \dots, (q-1)k\}$, the relevant contribution to GSD solely comes from $A_v^{(j)}$ and $B_e^{(0)}$ for

¹⁰The result (3.3) remains valid for the homomorphism with other choice of l , as long as Z_e^{ql} in the edge operator (see footnote 7) is not trivial for any $j \in \{1, 2, \dots, k-1\}$. Otherwise, matter fields with neutral electric charge appear, and the GSD would depend on other details of the graph in addition to $|V|$ and $|E|$.

all $v \in V$ and $e \in E$, making up $\prod_{v \in V} 1_v \prod_{e \in E} 1_e$. Note that for an edge e connecting two vertices v_1 and v_2 as in Fig 2, $A_{v_1}^{(j)} A_{v_2}^{(j)}$ acts trivially on \mathcal{H}_e . The last factor q on the second line counts the possible choice of j that is the number of $\prod_{v \in V} 1_v \prod_{e \in E} 1_e$'s.

3.2 Construction of ground states

If we find a seed state $|s\rangle$ satisfying $B_e|s\rangle = |s\rangle$ for any e , one of the ground states is given by

$$|\text{GS } s\rangle = \sqrt{\mathcal{N}} \left(\prod_{v \in V} A_v \right) |s\rangle, \quad (3.4)$$

where \mathcal{N} is a normalization constant. It is easy to see that $|s = 0\rangle \equiv \prod_{v \in V} |0_v\rangle \prod_{e \in E} |0_e\rangle$ gives such a state $|s\rangle$.

Starting with a ground state

$$|\text{GS } 0\rangle \equiv \sqrt{\mathcal{N}} \left(\prod_{v \in V} A_v \right) |s = 0\rangle, \quad (3.5)$$

we can exhaust the other ground states by acting the local operators $x_v^a \mathbf{X}_{L_v}^a$ ($a \in \mathbb{Z}_p$) and X_e^{bk} ($b \in \mathbb{Z}_q$) on $|s = 0\rangle$. Note that $x_v \mathbf{X}_{L_v}$ acts as a \mathbb{Z}_p -transformation on $|\text{GS } 0\rangle$ or on A_v , because of $x_v^p \mathbf{X}_{L_v}^p A_v = A_v$. However, all the choices are not independent. For

$$A_v^{(bk)} = 1_v \mathbf{X}_{L_v}^{pbk} \quad (3.6)$$

in (2.4), $A_v A_v^{(bk)} = A_v$ ($b \in \mathbb{Z}_q$) holds, which means that $|s_1\rangle$ and $|s_2\rangle$ such that $|s_1\rangle = A_v^{(bk)} |s_2\rangle$ for any b and v give the same ground state. Taking into account the constraint $\prod_{v \in V} A_v^{(bk)} = 1$, the number of the independent choices amounts to

$$\frac{p^{|V|} q^{|E|}}{q^{|V|-1}} = p^{|V|} q^{B_1} = \text{GSD}. \quad (3.7)$$

Alternatively, we pick edges \hat{e}_L ($L = 1, \dots, B_1$) such that the graph $T \equiv G - \{\hat{e}_1, \dots, \hat{e}_{B_1}\}$ becomes a connected tree graph, i.e., a spanning tree. Then, the independent ground states are generated by acting $x_v^{a_v} \mathbf{X}_{L_v}^{a_v}$ ($a_v \in \mathbb{Z}_p$, $v \in V$) and $X_{\hat{e}_L}^{b_L k}$ ($b_L \in \mathbb{Z}_q$, $L = 1, \dots, B_1$) on $|s = 0\rangle$. The states $|s\rangle$ giving the independent ground states are labelled by $\{a_v | v \in V\}$ and $\{b_L | L = 1, \dots, B_1\}$ for a choice of \hat{e}_L 's. The choice of \hat{e}_L 's is not unique. If one of the \hat{e}_L 's, say \hat{e}_1 , is added to the above spanning tree, a closed path including \hat{e}_1 appears. We can choose any other edge on the closed path instead of \hat{e}_1 . For example, in a graph depicted in Fig. 3, we

can choose one among e_{12} , e_{37} , e_{14} , e_{45} , e_{56} and e_{67} instead of \hat{e}_1 , where e_{ij} denotes the edge in T connecting the vertices v_i and v_j . The choice of the other \hat{e}_L 's can be changed similarly. We obtain the same set of independent ground states irrespective of the choice as we see below.

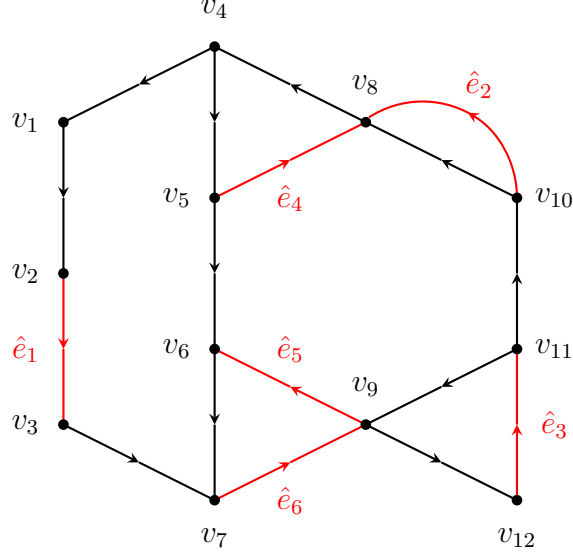


Figure 3: A graph with a choice of \hat{e}_L 's. The red lines with arrows represent \hat{e}_L ($L = 1, \dots, 6$), and the black lines with arrows represent the other edges. The black lines and the vertices form a spanning tree of the graph.

Noting that $A_v^{(bk)}$ acts on the vertex v as identity, the normalization is computed as¹¹

$$\begin{aligned} \langle \text{GS } s | \text{GS } s \rangle &= \mathcal{N} \langle s | \prod_{v \in V} A_v | s \rangle = \mathcal{N} \left(\frac{1}{n} \right)^{|V|} \langle s | \left(\prod_{v \in V} \sum_{b=0}^{q-1} A_v^{(bk)} \right) | s \rangle = \mathcal{N} n^{-|V|} \sum_{b=0}^{q-1} \langle s | \prod_{v \in V} A_v^{(bk)} | s \rangle \\ &= \mathcal{N} n^{-|V|} q, \end{aligned} \quad (3.8)$$

which determines \mathcal{N} as

$$\mathcal{N} = \frac{n^{|V|}}{q}. \quad (3.9)$$

Choice of \hat{e}_L 's Here, we show that the same set of the independent ground states is obtained irrespective of the choice of \hat{e}_L 's.

When we change the initial choice of one of \hat{e}_L 's, say \hat{e}_{L_0} , we choose an edge among the edges on the closed path in the graph $T + \{\hat{e}_{L_0}\}$, instead of \hat{e}_{L_0} . Suppose we pick an edge e'

¹¹Similar to the computation in the previous subsection, nonvanishing contribution arises only when the index b of $A_v^{(bk)}$ is the same for all v , which provides the last equality on the first line of (3.8).

instead of \hat{e}_{L_0} . Then the graph $T - \{e'\}$, the spanning tree T after the edge e' is removed, splits into two connected tree graphs, which are denoted by T_1 and T_2 . We can see that $\prod_{v \in T_1} A_v^{(bk)}$ becomes the product of $X_e^{\pm pbk}$'s with respect to the edges $e = \hat{e}_{L_0}$, e' and some other \hat{e}_L 's, where \pm in the power is fixed by the orientation. $\prod_{v \in T_2} A_v^{(bk)}$ gives essentially the same result, since $\prod_{v \in T_2} A_v^{(bk)} = \left(\prod_{v \in V} A_v^{(bk)} \right) \prod_{v \in T_1} A_v^{(-bk)} = \prod_{v \in T_1} A_v^{(-bk)}$.

Noting that

$$\{X_e^{bk} \mid b \in \mathbb{Z}_q\} = \{X_e^{pbk} \mid b \in \mathbb{Z}_q\} \quad (3.10)$$

due to $\gcd(p, q) = 1$, we label the state $|s\rangle$ by a_v 's and pb_L 's:

$$|s\rangle = \left(\prod_{v \in V} x_v^{a_v} \mathbf{X}_{L_v}^{a_v} \right) \left(\prod_{L=1}^{B_1} X_{\hat{e}_L}^{pb_L k} \right) |s = 0\rangle. \quad (3.11)$$

The above result leads to

$$\left(\prod_{v \in T_1} A_v^{(-b_{L_0} k)} \right) |s\rangle = \left(\prod_{v \in V} x_v^{a_v} \mathbf{X}_{L_v}^{a_v} \right) \left(\prod_{L \neq L_0} X_{\hat{e}_L}^{pb'_L k} \right) X_{e'}^{-pb_{L_0} k} |s = 0\rangle, \quad (3.12)$$

where $b'_L = b_L \pm b_{L_0}$ for the edge \hat{e}_L appearing in the result of $\prod_{v \in T_1} A_v^{(bk)}$, otherwise $b'_L = b_L$. In (3.12) e' appears with the label $-pb_{L_0}$ instead of \hat{e}_{L_0} , and some other \hat{e}_L 's remain with the label changed by $\pm pb_{L_0}$, compared to the initial choice (3.11). The RHS of (3.12) describes the seed state with the choice of \hat{e}_{L_0} changed to e' , and the LHS shows that it provides the same ground state as (3.11) as we saw below (3.6). Thus, we can say that the ground state is invariant under the change of \hat{e}_{L_0} accompanied with appropriate change of the labels $\{b_L\}$. Since the number of the labels $\{b_L\}$ does not change before and after the change of the choice, the set of the independent ground states remains the same.

Let us illustrate the above in the graph in Fig. 3. We consider the case $\hat{e}_{L_0} = \hat{e}_5$, and take $e' = e_{48}$ in the closed path on the graph $T + \hat{e}_5$. Then, $T - \{e_{48}\}$ splits into the two connected tree graphs: T_1 composed by the vertices v_1, \dots, v_7 and the black edges connecting them, and T_2 composed by v_8, \dots, v_{12} and the black edges connecting them. We have

$$\prod_{v \in T_1} A_v^{(bk)} = (X_{\hat{e}_5} X_{e_{48}} X_{\hat{e}_4}^{-1} X_{\hat{e}_6}^{-1})^{pbk}. \quad (3.13)$$

Acting $\prod_{v \in T_1} A_v^{(-b_5 k)}$ on the initial choice (3.11) with $B_1 = 6$ leads to

$$\left(\prod_{v \in T_1} A_v^{(-b_5 k)} \right) |s\rangle = \left(\prod_{v \in V} x_v^{a_v} \mathbf{X}_{L_v}^{a_v} \right) \left(\prod_{L=1}^3 X_{\hat{e}_L}^{pb_L k} \right) X_{\hat{e}_4}^{p(b_4+b_5)k} X_{\hat{e}_6}^{p(b_6+b_5)k} X_{e_{48}}^{-pb_5 k} |s = 0\rangle. \quad (3.14)$$

Thus, the ground state (3.4) remains the same under the change of \hat{e}_5 to e_{48} together with labels changed as $b_5 \rightarrow -b_5$, $b_4 \rightarrow b_4 + b_5$ and $b_6 \rightarrow b_6 + b_5 \pmod{q}$.

Since this procedure can be repeated for changes of the other \hat{e}_L 's, we can say that the same set of the independent ground states is obtained irrespective of the choice of \hat{e}_L 's.

The obtained ground states $|\text{GS } s\rangle$ in (3.4) and (3.11) with $s = 0, 1, \dots, (\text{GSD}) - 1$ are eigenstates of the local operator z_v^k ($\forall v \in V$) and the operator of quasi-local symmetry $Z(C)$ in (2.17) for any closed path C . Let C_L denote a closed path appearing when \hat{e}_L is added to the spanning tree T . $|\text{GS } s\rangle$ is distinguished by the eigenvalues of z_v^k 's and $Z(C_L)$'s which measure a_v 's and b_L 's respectively:

$$z_v^k |\text{GS } s\rangle = \omega_p^{a_v} |\text{GS } s\rangle, \quad (3.15)$$

$$Z(C_L) |\text{GS } s\rangle = \omega_q^{pb_L(\hat{e}_L|C_L)} |\text{GS } s\rangle. \quad (3.16)$$

In order to give a physical interpretation of (3.16), let us pick an embedding space of the graph in which a simply connected domain bounded by C_L can be defined.¹² From the analogy to the field theory in appendix A, a_v represents some degrees of freedom of the matter field ϕ at the point v on the ground state, while $pb_L(\hat{e}_L|C_L)$ is interpreted as magnetic flux penetrating the inside of C_L since the Wilson loop measures magnetic flux penetrating the domain surrounded by the loop. This is valid even if C_L is a topologically nontrivial cycle under the setting of the embedding space. Note that for any $L' (\neq L)$, $\hat{e}_{L'}$ does not belong to C_L , which is seen from the above definition of C_L . $U(1)$ gauge field on a circle has nontrivial topological structure as briefly summarized in appendix B. In particular, the nontrivial topological configuration of the gauge field generates magnetic flux as seen in (B.8), which is analogous to the twist by $X_{\hat{e}_L}^{pb_L k}$ providing the \mathbb{Z}_q magnetic flux pb_L .

On the other hand, an individual ground state is not invariant under the local transformations $x_v \mathbf{X}_{L_v}$ and X_e^k , but mapped to another individual ground state.

¹²Graphs consist of vertices and edges as mentioned in the beginning of section 2. Since the domain bounded by C_L lies outside the graph, we need to mention the embedding space in order to consider magnetic flux penetrating the domain. This is analogous to the global magnetic fluxes penetrating the hole of the torus in the toric code. Incidentally they also distinguish the ground states in the toric code just as how the local magnetic fluxes distinguish the ground states in our models.

3.3 Ground states $|\text{GS}[\alpha, \beta]\rangle$

Next, we construct eigenstates with respect to the local transformations $x_v \mathbf{X}_{L_v}$ and X_e^k by taking appropriate linear combinations of the ground states $|\text{GS } s\rangle$ ($s = 0, 1, \dots, (\text{GSD}) - 1$).

Let us introduce operators

$$P_v^{[\alpha_v]} \equiv \frac{1}{p} \sum_{a=0}^{p-1} \omega_p^{a\alpha_v} x_v^a \mathbf{X}_{L_v}^a \quad (\alpha_v \in \mathbb{Z}_p), \quad (3.17)$$

$$P_e^{[\beta_e]} \equiv \frac{1}{q} \sum_{b=0}^{q-1} \omega_q^{b\beta_e} X_e^{bk} \quad (\beta_e \in \mathbb{Z}_q). \quad (3.18)$$

Note that

$$P_v^{[\alpha_v]} = A_v P_v^{[\alpha_v]} = \frac{1}{np} \sum_{j=0}^{np-1} \omega_p^{j\alpha_v} x_v^j \mathbf{X}_{L_v}^j \quad (3.19)$$

holds on the ground states. As the RHSs of (3.18) and (3.19) show, they are projection operators on the ground states.

Acting the operator

$$\mathcal{P} = \mathcal{P}^{[\alpha, \beta]} \equiv \left(\prod_{v \in V} P_v^{[\alpha_v]} \right) \left(\prod_{L=1}^{B_1} P_{\hat{e}_L}^{[\beta_L]} \right). \quad (3.20)$$

on $|\text{GS } 0\rangle$ generates a desirable linear combination of all the ground states with the coefficients being phases:

$$|\text{GS}[\alpha, \beta]\rangle = \mathcal{P}|\text{GS } 0\rangle. \quad (3.21)$$

Compared with the ground states $|\text{GS } s\rangle$ in (3.4), the labels a_v 's and b_L 's are converted to α_v 's and β_L 's by the discrete Fourier transformations.

Associated to the ground state (3.21), we can regard the graph as an electric circuit in which the 'current' β_L flows on the line \hat{e}_L to the direction of its orientation. Then, the currents on the other lines which are not \hat{e}_L 's are determined by the 'current conservation' at the vertices. The current conservation follows from the relation $A_v^{(bk)} |\text{GS } s\rangle = |\text{GS } s\rangle$, namely

$$\prod_{e \in L_v^+} X_e^{pbk} = \prod_{e \in L_v^-} X_e^{pbk} \quad \text{on } |\text{GS } s\rangle \quad (3.22)$$

for any v and $b \in \mathbb{Z}_q$. We can see that

$$x_v \mathbf{X}_{L_v} |\text{GS}[\alpha, \beta]\rangle = \omega_p^{-\alpha_v} |\text{GS}[\alpha, \beta]\rangle, \quad (3.23)$$

$$X_e^k |\text{GS}[\alpha, \beta]\rangle = \begin{cases} \omega_q^{-\beta_L} |\text{GS}[\alpha, \beta]\rangle & (e = \hat{e}_L) \\ \omega_q^{-\bar{\beta}_e} |\text{GS}[\alpha, \beta]\rangle & (e \notin \{\hat{e}_1, \dots, \hat{e}_{B_1}\}), \end{cases} \quad (3.24)$$

where $\bar{\beta}_e$ represents the current on the edge e , a linear combination of β_L 's determined by the current conservation. Note that (3.18) can also be written as

$$P_e^{[\beta_e]} = \frac{1}{q} \sum_{b=0}^{q-1} \omega_q^{pb\beta_e} X_e^{pbk} \quad (\beta_e \in \mathbb{Z}_q) \quad (3.25)$$

since p and q are coprime. As an example, for the graph in Fig. 3, $\bar{\beta}_e$'s are determined as $\bar{\beta}_{e_{12}} = \bar{\beta}_{e_{14}} = \bar{\beta}_{e_{37}} = \beta_1$, $\bar{\beta}_{e_{67}} = -\beta_1 + \beta_6$, $\bar{\beta}_{e_{56}} = -\beta_1 - \beta_5 + \beta_6$, $\bar{\beta}_{e_{45}} = -\beta_1 + \beta_4 - \beta_5 + \beta_6$, $\bar{\beta}_{e_{48}} = \beta_4 - \beta_5 + \beta_6$, and so on.

By the discrete Fourier transformations of (3.11) and (3.12), we can see that when the choice of \hat{e}_{L_0} is changed to e' as discussed in the previous subsection, the initial ground state $|\text{GS}[\alpha, \beta]\rangle$ remains the same form with the current β_{L_0} on \hat{e}_{L_0} replaced to $\bar{\beta}_{e'}$ on e' . From a set of the ground states for any one choice of \hat{e}_L 's, the ground states for the other choices are derived.

Thus $|\text{GS}[\alpha, \beta]\rangle$ is invariant under the local \mathbb{Z}_p and \mathbb{Z}_q transformations (up to phase factors) as in (3.23) and (3.24). As A_v can be regarded as the Gauss law operator, $x_v^p \mathbf{X}_{L_v}^p$ corresponds to an operator of ‘small gauge transformations’, i.e., topologically trivial gauge transformations connected to the identity. Then, the local \mathbb{Z}_p and \mathbb{Z}_q transformations, which are not generated by $x_v^p \mathbf{X}_{L_v}^p$, can be interpreted as ‘large gauge transformations’, topologically nontrivial gauge transformations not connected to the identity. $|\text{GS}[\alpha, \beta]\rangle$ is similar to the θ vacuum in gauge theory when the vacuum has nontrivial topological structure, as seen in (B.6).

On the other hand, z_v^k and $Z(C_L)$ act on (3.21) as

$$z_v^k |\text{GS}[\alpha, \beta]\rangle = |\text{GS}[\tilde{\alpha}, \beta]\rangle, \quad (3.26)$$

$$Z(C_L) |\text{GS}[\alpha, \beta]\rangle = |\text{GS}[\alpha, \tilde{\beta}]\rangle, \quad (3.27)$$

where

$$\tilde{\alpha}_{v'} \equiv \begin{cases} \alpha_{v'} & (v' \neq v) \\ \alpha_v + 1 & (v' = v) \end{cases} \quad \text{and} \quad \tilde{\beta}_{L'} \equiv \begin{cases} \beta_{L'} & (L' \neq L) \\ \beta_L + (\hat{e}_L | C_L) & (L' = L). \end{cases} \quad (3.28)$$

From the analogy to the field theory in appendix A, α_v represents some degrees of freedom of the momentum π of the matter field at the point v on the ground state, while β_L is interpreted as electric flux or current flowing along \hat{e}_L since the Wilson loop creates the unit electric flux along the loop.¹³

¹³We can say that the two ground states $|\text{GS}s\rangle$ and $|\text{GS}[\alpha, \beta]\rangle$ are complementary in the sense of quantum

Norm of the ground state $|\mathbf{GS}[\alpha, \beta]\rangle$ Since the operator (3.20) satisfies $\mathcal{P} = \mathcal{P}^\dagger$, $\mathcal{P}^2 = \mathcal{P}$ and commutes with A_v for any v ,

$$\begin{aligned} \langle \mathbf{GS}[\alpha, \beta] | \mathbf{GS}[\alpha, \beta] \rangle &= \mathcal{N} \langle s = 0 | \left(\prod_{v \in V} A_v \right) \mathcal{P} | s = 0 \rangle \\ &= \mathcal{N} \left(\prod_{e \in E} \langle 0_e | \right) \left\{ \prod_{v \in V} \langle 0_v | A_v P_v^{[\alpha v]} | 0_v \rangle \right\} \left(\prod_{L=1}^{B_1} P_{\hat{e}_L}^{[\beta L]} \right) \left(\prod_{e \in E} | 0_e \rangle \right). \end{aligned} \quad (3.29)$$

Then,

$$\langle 0_v | A_v P_v^{[\alpha v]} | 0_v \rangle = \langle 0_v | A_v (P_v^{[\alpha v]})^\dagger | 0_v \rangle = \frac{1}{np} \sum_{j=0}^{n-1} \sum_{a=0}^{p-1} \omega_p^{-a\alpha v} \mathbf{X}_{L_v}^{pj-a} \delta_m(pj, a), \quad (3.30)$$

where $\langle 0_v | x_v^{pj-a} | 0_v \rangle$ gives $\delta_m(pj, a)$. The nonzero contribution comes from $a = 0$ and $j = ku$ ($u = 0, 1, \dots, q-1$), which leads to

$$\langle 0_v | A_v P_v^{[\alpha v]} | 0_v \rangle = \frac{1}{np} \sum_{j=0}^{q-1} \mathbf{X}_{L_v}^{kpj}, \quad (3.31)$$

and then

$$\langle \mathbf{GS}[\alpha, \beta] | \mathbf{GS}[\alpha, \beta] \rangle = \mathcal{N} \left(\frac{1}{np} \right)^{|V|} \left(\prod_{e \in E} \langle 0_e | \right) \left(\prod_{v \in V} \sum_{j=0}^{q-1} \mathbf{X}_{L_v}^{kpj} \right) \left(\prod_{L=1}^{B_1} P_{\hat{e}_L}^{[\beta L]} \right) \left(\prod_{e \in E} | 0_e \rangle \right). \quad (3.32)$$

In evaluating this, we combine the results

$$\langle 0_e | X_e^{kpj} X_e^{-kpj'} | 0_e \rangle = \delta_q(j, j') \quad (3.33)$$

and¹⁴

$$\langle 0_{\hat{e}_L} | X_{\hat{e}_L}^{kpj} X_{\hat{e}_L}^{-kpj'} P_{\hat{e}_L}^{[\beta L]} | 0_{\hat{e}_L} \rangle = \frac{1}{q} \omega_q^{\beta L p(j'-j)}. \quad (3.34)$$

theory. Namely, they are analogous to the position eigenstate $|x\rangle$ and the momentum eigenstate $|p\rangle$ with the commutation relation of the corresponding operators $[\hat{x}, \hat{p}] = i$. The relation $|p\rangle = \int dx e^{ipx} |x\rangle$ is similar to the ground states related by the discrete Fourier transformations. The operator $e^{ia\hat{x}}$, which is analogous to z_v^k or $Z(C_L)$, measures the position when it acts on the position eigenstate, whereas it creates a shift of the momentum when it acts on the momentum eigenstate.

¹⁴(3.34) is derived as follows. Using (3.25), the LHS becomes

$$\frac{1}{q} \sum_{b=0}^{q-1} \omega_q^{bp\beta L} \langle 0_{\hat{e}_L} | X_{\hat{e}_L}^{kp(j-j'+b)} | 0_{\hat{e}_L} \rangle = \frac{1}{q} \sum_{b=0}^{q-1} \omega_q^{bp\beta L} \delta_n(kp(j-j'+b), 0).$$

The mod n Kronecker delta is nonzero only when $b = j' - j \pmod{q}$, which gives the RHS of (3.34).

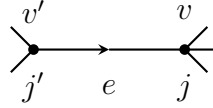


Figure 4: The indices j and j' in the figure represents the operators $\mathbf{X}_{L_v}^{kpj}$ and $\mathbf{X}_{L_{v'}}^{kpj'}$ sitting at the vertices v and v' , respectively. The edge e connects the vertices. These operators yield the operators in the LHS of eq.(3.33). The result of (3.33) shows that only the case $j = j' \pmod{q}$ is relevant.

Let us first consider (3.33) for $e \in E - \{\hat{e}_1, \dots, \hat{e}_{B_1}\}$. As seen in Fig. 4, The indices j and j' are associated to the vertices v and v' at both ends of the edge e . For giving nonzero contribution, j and j' should be equal \pmod{q} . From the fact that the graph $T = G - \{\hat{e}_1, \dots, \hat{e}_{B_1}\}$ is a connected tree graph, all the vertices are connected by the mod q Kronecker delta (3.33), which makes all the indices j equal. Then ω_q -factor in (3.34) becomes 1. Finally we have

$$\langle \text{GS}[\alpha, \beta] | \text{GS}[\alpha, \beta] \rangle = \mathcal{N} \left(\frac{1}{np} \right)^{|V|} \left(\sum_{j=0}^{q-1} 1 \right) \frac{1}{q^{B_1}} = \frac{1}{\text{GSD}}, \quad (3.35)$$

where we used (3.9).

Pure-state density matrix Next, when \mathcal{P} in (3.20) acts on other $|\text{GS } s\rangle$ with $s \neq 0$, it also gives $|\text{GS}[\alpha, \beta]\rangle$ up to some phase factors:

$$\mathcal{P}|\text{GS } s\rangle = e^{i\theta_s} |\text{GS}[\alpha, \beta]\rangle, \quad (3.36)$$

which leads to

$$\mathcal{P}|\text{GS } s\rangle \langle \text{GS } s| \mathcal{P}^\dagger = |\text{GS}[\alpha, \beta]\rangle \langle \text{GS}[\alpha, \beta]| \quad (3.37)$$

for any s .

Finally, we find that the desired pure-state density matrix is given by the \mathcal{P} transformation to the projector (3.1), $\pi_0 = \prod_{v \in V} A_v \prod_{e \in E} B_e = \sum_{s=0}^{(\text{GSD})-1} |\text{GS } s\rangle \langle \text{GS } s|$:

$$\rho^{[\alpha, \beta]} \equiv \mathcal{P} \pi_0 \mathcal{P}^\dagger = \sum_{s=0}^{(\text{GSD})-1} \mathcal{P} |\text{GS } s\rangle \langle \text{GS } s| \mathcal{P}^\dagger = (\text{GSD}) \times |\text{GS}[\alpha, \beta]\rangle \langle \text{GS}[\alpha, \beta]|. \quad (3.38)$$

(3.35) means that $\rho^{[\alpha, \beta]}$ has the correct normalization $\text{Tr } \rho^{[\alpha, \beta]} = 1$. From the properties of \mathcal{P} , $\rho^{[\alpha, \beta]}$ is simplified as

$$\rho^{[\alpha, \beta]} = \left(\prod_{v \in V} A_v \prod_{e \in E} B_e \right) \mathcal{P}. \quad (3.39)$$

4 Entanglement Entropy

To better understand the ground states of the Hamiltonian (2.13), we compute their EE. As the system is gapped, we expect that the leading order term is proportional to the ‘area’ of the boundary of a bipartition of the system (the *area law*), which is proven in gapped one-dimensional systems [34]. Further interesting features are expected in a constant sub-leading term, called *topological EE* [5, 35–38], which is a speculated signal for a topologically ordered state. This is a global term to the EE that is present regardless of the partition of the system.

In this section, we exactly compute the EE (and thus the topological EE) both for the individual ground states $|\text{GS } s\rangle$ and their linear combinations $|\text{GS}[\alpha, \beta]\rangle$, with respect to a bipartite separation of the system. We first split the total system given by the graph G into the three parts:

$$G = G_1 + G_2 + E_{12}, \quad (4.1)$$

where each of G_1 and G_2 is a connected subgraph, and E_{12} is a set of edges connecting G_1 (at the vertices ν_1, \dots, ν_r) and G_2 (at the vertices $\bar{\nu}_1, \dots, \bar{\nu}_{r'}$). An example of the division (4.1) is depicted in Fig. 5. N_v and N_e denote the numbers of vertices and edges of G_1 , and M_v and

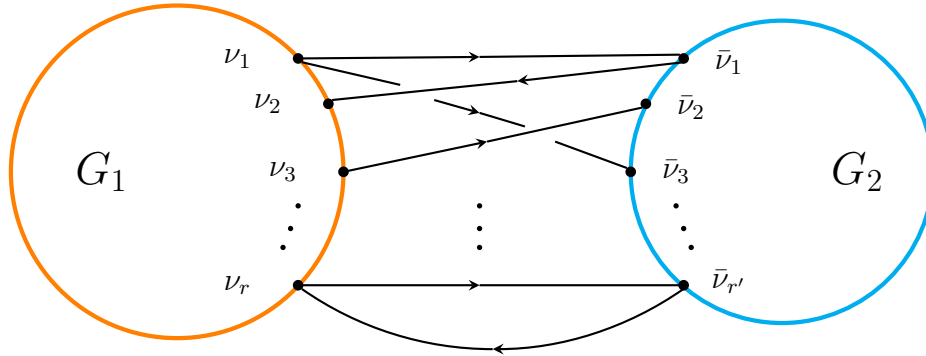


Figure 5: An example of the division (4.1). The orange (light blue) circle and its interior represent the region where the connected subgraph G_1 (G_2) is located. Edges and vertices in the interior are suppressed. The black lines with arrows are edges belonging to E_{12} , which connect G_1 at the vertices $\nu_1, \nu_2, \dots, \nu_r$ and G_2 at the vertices $\bar{\nu}_1, \bar{\nu}_2, \dots, \bar{\nu}_{r'}$.

M_e denote those of G_2 . E_{12} consists of f edges. Then, the first Betti numbers of G_1 and G_2 are given by

$$B'_1 = N_e - N_v + 1 \quad \text{and} \quad B''_1 = M_e - M_v + 1, \quad (4.2)$$

respectively. Then the first Betti number of G is

$$B_1 = |E| - |V| + 1 = (N_e + M_e + f) - (N_v + M_v) + 1 = B'_1 + B''_1 + f - 1. \quad (4.3)$$

For computing the bipartite EE, we take a subsystem A as G_1 and trace out the degrees of freedom of the rest $B = G_2 + E_{12}$. For each $t = 1, \dots, r$, we divide a set of the edges attaching to the vertex ν_t , $L_t (\equiv L_{\nu_t})$,¹⁵ into a set of those belonging to G_1 , $L'_t (= L_t \cap G_1)$, and a set of those belonging to E_{12} , $\tilde{L}_t (= L_t \cap E_{12})$:

$$L_t = L'_t + \tilde{L}_t \quad (t = 1, \dots, r). \quad (4.4)$$

Likewise, for $\bar{t} = \bar{1}, \dots, \bar{r}'$, $L_{\bar{t}} (\equiv L_{\bar{\nu}_t})$ is divided into $L'_{\bar{t}} (= L_{\bar{t}} \cap G_2)$ and $\tilde{L}_{\bar{t}} (= L_{\bar{t}} \cap E_{12})$:

$$L_{\bar{t}} = L'_{\bar{t}} + \tilde{L}_{\bar{t}} \quad (\bar{t} = \bar{1}, \dots, \bar{r}'). \quad (4.5)$$

Correspondingly, \mathbf{X}_{L_t} and $\mathbf{X}_{L_{\bar{t}}}$ are factored as

$$\mathbf{X}_{L_t} = \mathbf{X}_{L'_t} \mathbf{X}_{\tilde{L}_t} \quad (t = 1, \dots, r) \quad \text{and} \quad \mathbf{X}_{L_{\bar{t}}} = \mathbf{X}_{L'_{\bar{t}}} \mathbf{X}_{\tilde{L}_{\bar{t}}} \quad (\bar{t} = \bar{1}, \dots, \bar{r}'). \quad (4.6)$$

Then, $E_{12} = \{\tilde{L}_1, \dots, \tilde{L}_r\} = \{\tilde{L}_{\bar{1}}, \dots, \tilde{L}_{\bar{r}'}\}$. For any edge connecting the vertices $\nu_t \in G_1$ and $\bar{\nu}_{t'} \in G_2$, when the edge is incoming to ν_t , it is outgoing from $\bar{\nu}_{t'}$, and vice versa. Thus,

$$\prod_{t=1}^r \mathbf{X}_{\tilde{L}_t} = \prod_{\bar{t}=\bar{1}}^{\bar{r}'} \mathbf{X}_{\tilde{L}_{\bar{t}}}^{-1} \quad (4.7)$$

holds.

4.1 Bipartite EE for $|\text{GS } s\rangle$

We start with a pure state described by the density matrix

$$\rho_s = |\text{GS } s\rangle \langle \text{GS } s| \quad \text{with} \quad s = 0, 1, \dots, (\text{GSD}) - 1, \quad (4.8)$$

and compute the reduced density matrix by tracing out the degrees of freedom of $B = G_2 + E_{12}$:

$$\rho_{s,A} = \text{Tr}_B \rho_s = \frac{n^{N_v + M_v}}{q} \text{Tr}_B \left[\left(\prod_{v \in V} A_v \right) |s\rangle \langle s| \left(\prod_{v \in V} A_v \right) \right], \quad (4.9)$$

¹⁵In this section, we often write the subscripts ν_t ($t = 1, \dots, r$) and $\bar{\nu}_t$ ($t = 1, \dots, r'$) as t and \bar{t} for notational simplicity. Then \bar{t} runs over $\bar{1}, \dots, \bar{r}'$.

where (3.4) and (3.9) are used. On the RHS of

$$\prod_{v \in V} A_v = \left(\prod_{v \in G_1 - \{\nu_1, \dots, \nu_r\}} A_v \right) \left(\prod_{t=1}^r A_t \right) \left(\prod_{v \in G_2} A_v \right), \quad (4.10)$$

the first factor is irrelevant to the trace, whereas the last factor is fully traced out and the trace cyclicity can be applied. $|s\rangle$ in (3.11) can be expressed as a product state

$$|s\rangle = \prod_{v \in V} |h_v\rangle \prod_{e \in E} |i_e\rangle \quad \text{for some } h_v \in \mathbb{Z}_m, i_e \in \mathbb{Z}_n \quad (4.11)$$

which is similarly decomposed. Then (4.9) reads

$$\rho_{s,A} = \frac{n^{N_v+M_v}}{q} \mathcal{A}_1 \text{Tr}_B \left[\mathcal{A}_{\text{bdy}} \left(\prod_{v \in G_2} A_v |h_v\rangle \langle h_v| \right) \left(\prod_{e \in B} |i_e\rangle \langle i_e| \right) \mathcal{A}_{\text{bdy}}^\dagger \right] \mathcal{A}_1^\dagger \quad (4.12)$$

with

$$\mathcal{A}_1 \equiv \left(\prod_{v \in G_1 - \{\nu_1, \dots, \nu_r\}} A_v \right) \left(\prod_{e \in G_1 - \{L'_1, \dots, L'_r\}} |i_e\rangle \right), \quad (4.13)$$

$$\mathcal{A}_{\text{bdy}} \equiv \prod_{t=1}^r A_t |h_t\rangle |i_{L'_t}\rangle, \quad |i_{L'_t}\rangle \equiv \prod_{e \in L'_t} |i_e\rangle. \quad (4.14)$$

Note that \mathcal{A}_1 and \mathcal{A}_{bdy} act nontrivially on the Hilbert space on $e \in \{L'_1, \dots, L'_r\} \subset G_1$ and that on $e \in \{\tilde{L}_1, \dots, \tilde{L}_r\} = E_{12}$, respectively.

Computation of Tr_{G_2} In the computation of $\text{Tr}_B = \text{Tr}_{E_{12}} \text{Tr}_{G_2}$, let us first compute $\text{Tr}_{v \in G_2}$ and then $\text{Tr}_{e \in G_2}$.

The relevant part of the former is only the second factor in $\text{Tr}_B[\dots]$ in (4.12):

$$\text{Tr}_{v \in G_2} \left[\prod_{v \in G_2} A_v |h_v\rangle \langle h_v| \right] = \prod_{v \in G_2} \langle h_v | A_v | h_v \rangle = \left(\frac{1}{n} \right)^{M_v} \prod_{v \in G_2} \sum_{b=0}^{q-1} \mathbf{X}_{L_v}^{pbk}. \quad (4.15)$$

As is seen in (3.6), only $j = bk$ ($b \in \mathbb{Z}_q$) terms in (2.4) give nonvanishing contribution. Next, $\text{Tr}_{e \in G_2}$ is computed as

$$\begin{aligned} \text{Tr}_{e \in G_2} \left[\left(\prod_{v \in G_2} \sum_{b=0}^{q-1} \mathbf{X}_{L_v}^{pbk} \right) \left(\prod_{e \in G_2} |i_e\rangle \langle i_e| \right) \right] &= \left(\prod_{e \in G_2} \langle i_e| \right) \left(\prod_{v \in G_2} \sum_{b=0}^{q-1} \mathbf{X}_{L_v}^{pbk} \right) \left(\prod_{e \in G_2} |i_e\rangle \right) \\ &= \sum_{b=0}^{q-1} \prod_{\tilde{t}=1}^{\tilde{r}} \mathbf{X}_{\tilde{L}_{\tilde{t}}}^{pbk} = \sum_{b=0}^{q-1} \prod_{t=1}^r \mathbf{X}_{L'_t}^{pbk}, \end{aligned} \quad (4.16)$$

where (4.7) and the change of the summation index $b \rightarrow q - b$ were used at the last equality.

Now we find

$$\rho_{s,A} = \frac{n^{N_v}}{q} \mathcal{A}_1 \text{Tr}_{E_{12}} \left[\mathcal{A}_{\text{bdy}} \left(\sum_{b=0}^{q-1} \prod_{t=1}^r \mathbf{X}_{\tilde{L}_t}^{pbk} \right) \left(\prod_{e \in E_{12}} |i_e\rangle \langle i_e| \right) \mathcal{A}_{\text{bdy}}^\dagger \right] \mathcal{A}_1^\dagger. \quad (4.17)$$

Computation of $\text{Tr}_{E_{12}}$ From (4.4), $A_t (\equiv A_{\nu_t})$ can be expressed as $A_t = \frac{1}{n} \sum_{j=0}^{n-1} x_t^{pj} \mathbf{X}_{L'_t}^{pj} \mathbf{X}_{\tilde{L}_t}^{pj}$. $\text{Tr}_{E_{12}}[\dots]$ in (4.17) becomes

$$\begin{aligned} (\text{Tr}_{E_{12}}[\dots]) \text{ in (4.17)} &= \sum_{b=0}^{q-1} \prod_{t=1}^r \left\{ \left(\frac{1}{n} \right)^2 \sum_{j,j'=0}^{n-1} x_t^{pj} |h_t\rangle \mathbf{X}_{L'_t}^{pj} |i_{L'_t}\rangle \right. \\ &\times \text{Tr}_{\tilde{L}_t} \left[\mathbf{X}_{\tilde{L}_t}^{pj+pbk} \left(\prod_{e \in \tilde{L}_t} |i_e\rangle \langle i_e| \right) \mathbf{X}_{\tilde{L}_t}^{-pj'} \right] \left. \langle i_{L'_t} | \mathbf{X}_{L'_t}^{-pj'} \langle h_t | x_t^{-pj'} \right\}, \end{aligned} \quad (4.18)$$

in which $\text{Tr}_{\tilde{L}_t}[\dots]$ gives $\delta_n(p(-j' + j + bk), 0)$. From (2.3), the Kronecker delta means that $\tilde{p}(-j' + j + bk) = 0 \pmod{\tilde{k}q}$. Note that $\gcd(p, q) = \gcd(\xi\tilde{p}, q) = 1$ is equivalent to $\gcd(\xi, q) = 1$ and $\gcd(\tilde{p}, q) = 1$. Combining this and (2.3), we find $\gcd(\tilde{p}, \tilde{k}q) = 1$. Thus, j' giving nonzero contribution is $j' = j + bk \pmod{\tilde{k}q}$, i.e.,

$$j' = j + bk - \tilde{k}qu \quad (u \in \mathbb{Z}_\xi), \quad (4.19)$$

which leads to

$$(\text{Tr}_{E_{12}}[\dots]) \text{ in (4.17)} = \left(\sum_{b=0}^{q-1} \prod_{t=1}^r \mathbf{X}_{L'_t}^{-pbk} \right) \prod_{t=1}^r \left\{ \frac{\xi}{n^2} \left(\sum_{j=0}^{n-1} P_{t,j} P_{L'_t,j} \right) Q_t \right\}. \quad (4.20)$$

Here $P_{t,j}$, $P_{L'_t,j}$ and Q_t are projection operators defined by

$$P_{t,j} \equiv x_t^{pj} |h_t\rangle \langle h_t | x_t^{-pj}, \quad P_{L'_t,j} \equiv \mathbf{X}_{L'_t}^{pj} |i_{L'_t}\rangle \langle i_{L'_t} | \mathbf{X}_{L'_t}^{-pj}, \quad Q_t \equiv \frac{1}{\xi} \sum_{u=0}^{\xi-1} x_t^{p\tilde{k}qu}. \quad (4.21)$$

In deriving (4.20), $pbk = mb$ and $p\tilde{k}qu = \tilde{p}kqu = \tilde{p}nu$ were used.

Since it can be seen that the property

$$(P_{t,j} P_{L'_t,j}) (P_{t,j'} P_{L'_t,j'}) = \delta_{j,j'} (P_{t,j} P_{L'_t,j}) \quad (4.22)$$

holds, we introduce more projection operators as

$$P_t \equiv \sum_{j=0}^{n-1} P_{t,j} P_{L'_t,j}, \quad Q' \equiv \frac{1}{q} \sum_{b=0}^{q-1} \prod_{t=1}^r \mathbf{X}_{L'_t}^{-pbk}, \quad (4.23)$$

and obtain

$$(\text{Tr}_{E_{12}}[\cdots] \text{ in (4.17)}) = \left(\frac{\xi}{n^2}\right)^r q Q' \left(\prod_{t=1}^r P_t Q_t\right). \quad (4.24)$$

Plugging (4.24) to (4.17), we end up with

$$\rho_{s,A} = n^{N_v-2r} \xi^r \mathcal{A}_1 Q' \left(\prod_{t=1}^r P_t Q_t\right) \mathcal{A}_1^\dagger. \quad (4.25)$$

Notice that the projection operators Q' , P_t and Q_t mutually commute. $P_t x_t^{p\tilde{k}qu} = x_t^{p\tilde{k}qu} P_t$ and $P_t \mathbf{X}_{L'_t}^{-pbk} = \mathbf{X}_{L'_t}^{-pbk} P_t$ are verified by shifting j in the sum in the definition of P_t (4.23) as $j \rightarrow j + \tilde{k}qu$ and $j \rightarrow j - bk$, respectively. This leads to $P_t Q_t = Q_t P_t$ and $P_t Q' = Q' P_t$.

Bipartite EE A similar computation of (4.15) and (4.16) gives

$$\mathcal{A}_1^\dagger \mathcal{A}_1 = n^{-N_v+r} \sum_{b=0}^{q-1} \prod_{t=1}^r \mathbf{X}_{L'_t}^{-pbk} = n^{-N_v+r} q Q'. \quad (4.26)$$

Then we find

$$\rho_{s,A}^2 = \tilde{n}^{-r} q \rho_{s,A} \quad (4.27)$$

with (2.16). It means $\text{Spec } \rho_{s,A} = \{\tilde{n}^{-r} q, 0\}$. As it should be from $\text{Tr } \rho_s = 1$, we can directly check $\text{Tr } \rho_{s,A} = 1$ from the expression (4.25). Thus, it is seen that $\rho_{s,A}$ has the eigenvalue $\tilde{n}^{-r} q$ with multiplicity $\tilde{n}^r q^{-1}$.

Finally, the bipartite EE is obtained as

$$\begin{aligned} S_{s,A} &= -\text{Tr} [\rho_{s,A} \log_2 \rho_{s,A}] = -\{(\tilde{n}^{-r} q) \log_2 (\tilde{n}^{-r} q)\} \times \tilde{n}^r q^{-1} \\ &= (\log_2 \tilde{n}) r - \log_2 q. \end{aligned} \quad (4.28)$$

The result (4.28) is independent of a_v 's and b_L 's which labels the state $|s\rangle$. Namely, all the individual ground state $|\text{GS } s\rangle$ gives the same EE. As r grows the linear term of r dominates, which shows that contribution around the boundary between the subsystems becomes dominant in the EE. Namely the EE obeys the area law. On the other hand, the constant term $-\log_2 q$ characterizes a global feature of the entanglement of the ground state, which is called the topological EE [5].¹⁶ The topological EE is denoted by $-\gamma$. Here we have

$$\gamma = \log_2 q \quad (4.29)$$

¹⁶In [5, 38], prescriptions are presented to obtain the constant contribution eliminating the short range effects, in which it is not necessary to identify the linear term to be subtracted from the whole expression.

and the total quantum dimension is $D = q$. For $q = 1$ (m is an integer multiple of n : $m = pn$), the topological EE vanishes.

For $r \geq 2$, (4.28) vanishes only when $\tilde{k} = q = 1$ (i.e., m is an integer multiple of n^2 : $m = \tilde{p}n^2$). Then, the vertex operator A_v reduces to a strictly local operator (nontrivially acting only on the vertex v): $A_v = \frac{1}{\xi} \sum_{j=0}^{\xi-1} x_v^{\xi \tilde{p} j} 1_{L_v}$. Since the A_v does not generate entanglement, the ground state (3.4) becomes a product state.

The ground states $|\text{GS } s\rangle$ have definite magnetic flux for each independent closed path on the graph. This corresponds to the basis state which maximizes the negative of the topological EE, γ , according to [30,31]. However, in the next subsection we will see that it does not always mean minimizing the whole EE, which is the case in the toric code [30,31].

4.2 Bipartite EE for $\rho^{[\alpha, \beta]}$

In the computation of the EE for the density matrix (3.39), let us consider the case that among the \hat{e}_L 's, the first B'_1 , $\{\hat{e}_1, \dots, \hat{e}_{B'_1}\}$, are in G_1 , the next B''_1 , $\{\hat{e}_{B'_1+1}, \dots, \hat{e}_{B'_1+B''_1}\}$, in G_2 , and the rest, $\{\hat{e}_{B'_1+B''_1+1}, \dots, \hat{e}_{B_1}\}$, in E_{12} . From (4.3), we see that $(f-1)$ of the f edges of E_{12} are \hat{e}_L 's. Notice that any choice of \hat{e}_L 's can be reduced to the case as discussed in section 3.3.

The reduced density matrix reads

$$\begin{aligned} \rho_A^{[\alpha, \beta]} &= \text{Tr}_B \rho^{[\alpha, \beta]} = \text{Tr}_B \left[\left(\prod_v A_v P_v^{[\alpha_v]} \right) \left(\prod_e B_e \right) \left(\prod_{L=1}^{B_1} P_{\hat{e}_L}^{[\beta_L]} \right) \right] \\ &= \left(\prod_{v \in G_1 - \{\nu_1, \dots, \nu_r\}} A_v P_v^{[\alpha_v]} \right) \left(\prod_{e \in G_1} B_e \right) \left(\prod_{L=1}^{B'_1} P_{\hat{e}_L}^{[\beta_L]} \right) \\ &\quad \times \text{Tr}_B \left[\left(\prod_{t=1}^r A_t P_t^{[\alpha_t]} \right) \left(\prod_{v \in G_2} A_v P_v^{[\alpha_v]} \right) \left(\prod_{e \in B} B_e \right) \left(\prod_{L=B'_1+1}^{B_1} P_{\hat{e}_L}^{[\beta_L]} \right) \right]. \end{aligned} \quad (4.30)$$

Here it is easy to see that for $(\prod_{e \in B} B_e)$ only $\frac{1}{k} B_e^{(0)}$ in B_e (2.9) gives nonzero contribution. So we may replace $(\prod_{e \in B} B_e)$ with the factor $k^{-M_e - f}$. The last line of (4.30) becomes

$$\begin{aligned} (\text{last line of (4.30)}) &= k^{-M_e - f} \text{Tr}_{E_{12}} \left\{ \left(\prod_{t=1}^r A_t P_t^{[\alpha_t]} \right) \left(\prod_{L=B'_1+B''_1+1}^{B_1} P_{\hat{e}_L}^{[\beta_L]} \right) \right. \\ &\quad \left. \times \text{Tr}_{G_2} \left[\left(\prod_{v \in G_2} A_v P_v^{[\alpha_v]} \right) \left(\prod_{L=B'_1+1}^{B'_1+B''_1} P_{\hat{e}_L}^{[\beta_L]} \right) \right] \right\}. \end{aligned} \quad (4.31)$$

Computation of Tr_{G_2} For the computation of Tr_{G_2} in (4.31), we first evaluate $\text{Tr}_{v \in G_2}$ and then $\text{Tr}_{e \in G_2}$.

In a similar manner to (3.31),

$$\text{Tr}_v (A_v P_v^{[\alpha_v]}) = \frac{1}{q} \sum_{j=0}^{q-1} \mathbf{X}_{L_v}^{k p j}, \quad (4.32)$$

which leads to

$$(\text{Tr}_{G_2}[\cdots] \text{ in (4.31)}) = q^{-M_v} \text{Tr}_{e \in G_2} \left[\prod_{v \in G_2} \left(\sum_{j=0}^{q-1} \mathbf{X}_{L_v}^{k p j} \right) \cdot \left(\prod_{L=B'_1+1}^{B'_1+B''_1} P_{\hat{e}_L}^{[\beta_L]} \right) \right]. \quad (4.33)$$

Similar to (3.33) and (3.34),

$$\text{Tr}_e \left(X_e^{k p j} X_e^{-k p j'} \right) = n \delta_q(j, j'), \quad (4.34)$$

$$\text{Tr}_{\hat{e}_L} \left(X_{\hat{e}_L}^{k p j} X_{\hat{e}_L}^{-k p j'} P_{\hat{e}_L}^{[\beta_L]} \right) = \frac{n}{q} \omega_q^{\beta_L p(j'-j)}. \quad (4.35)$$

Since the graph $G_2 - \{\hat{e}_{B'_1+1}, \dots, \hat{e}_{B'_1+B''_1}\}$ becomes a connected tree graph, all the j -indices become the same due to the mod q Kronecker delta (4.34) from each edge, and the ω_q -factors from (4.35) all become 1. Then we find

$$(\text{Tr}_{G_2}[\cdots] \text{ in (4.31)}) = n^{M_e} q^{-M_v - B''_1} \sum_{j=0}^{q-1} \prod_{t=1}^{r'} \mathbf{X}_{\tilde{L}_t}^{k p j}, \quad (4.36)$$

where (4.5) and (4.6) are used.

Plugging (4.36) to (4.31) we have

$$(\text{last line of (4.30)}) = k^{-f} q^{-1} \text{Tr}_{E_{12}} \left\{ \left(\prod_{t=1}^r A_t P_t^{[\alpha_t]} \right) \left(\prod_{L=B'_1+B''_1+1}^{B_1} P_{\hat{e}_L}^{[\beta_L]} \right) \sum_{j=0}^{q-1} \prod_{t=1}^r \mathbf{X}_{\tilde{L}_t}^{-k p j} \right\}, \quad (4.37)$$

after (4.2) and (4.7) are used.

Computation of $\text{Tr}_{E_{12}}$ Using (3.19) and (4.6), we express (4.37) as

$$\begin{aligned} (\text{last line of (4.30)}) &= k^{-f} q^{-1} (np)^{-r} \sum_{j'=0}^{q-1} \sum_{j_1, \dots, j_r=0}^{np-1} \left(\prod_{t=1}^r \omega_p^{j_t \alpha_t} x_t^{j_t} \mathbf{X}_{L'_t}^{j_t} \right) \\ &\quad \times \text{Tr}_{E_{12}} \left\{ \left(\prod_{t=1}^r \mathbf{X}_{\tilde{L}_t}^{j_t - k p j'} \right) \left(\prod_{L=B'_1+B''_1+1}^{B_1} P_{\hat{e}_L}^{[\beta_L]} \right) \right\}. \end{aligned} \quad (4.38)$$

Note that j_t is associated to the vertex ν_t and j' is associated to the vertices $\bar{\nu}_1, \dots, \bar{\nu}_{r'}$.

Computation of the trace on each edge goes as

$$\mathrm{Tr}_e \left(X_e^{-j_t} X_e^{kpj'} \right) = n \delta_n(j_t, kpj'), \quad (4.39)$$

from which j_t giving nonzero contribution is

$$j_t = kpj' + kqu \pmod{np} \quad (4.40)$$

with $j' = 0, 1, \dots, q-1$ and $u = 0, 1, \dots, p-1$. Also,

$$\mathrm{Tr}_{\hat{e}_L} \left(X_{\hat{e}_L}^{-j_t} X_{\hat{e}_L}^{kpj'} P_{\hat{e}_L}^{[\beta_L]} \right) = \frac{1}{q} \sum_{b=0}^{q-1} \omega_q^{b\beta_L} \mathrm{Tr}_{\hat{e}_L} X_{\hat{e}_L}^{-j_t + kpj' + bk} = \frac{n}{q} \sum_{b=0}^{q-1} \omega_q^{b\beta_L} \delta_n(j_t, k(b + pj')). \quad (4.41)$$

Here, j_t giving nonzero contribution is

$$j_t = k\tilde{j}_t \quad (\tilde{j}_t = 0, 1, \dots, pq-1), \quad (4.42)$$

and then we find

$$\mathrm{Tr}_{\hat{e}_L} \left(X_{\hat{e}_L}^{-j_t} X_{\hat{e}_L}^{kpj'} P_{\hat{e}_L}^{[\beta_L]} \right) = \frac{n}{q} \omega_q^{\beta_L(\tilde{j}_t - pj')}. \quad (4.43)$$

As mentioned above, $(f-1)$ of the f edges in E_{12} are \hat{e}_L 's. We assume that the only one edge in E_{12} which is not \hat{e}_L attaches to the vertex ν_1 . It does not lose generality, since this situation can be always realized by appropriately renaming the vertices ν_1, \dots, ν_r .

Plugging (4.39)-(4.43) to (4.38) leads to

$$\begin{aligned} \text{(last line of (4.30))} &= (np)^{-r} \sum_{j'=0}^{q-1} \sum_{u=0}^{p-1} \omega_p^{kq\alpha_1 u} x_1^{kqu} \mathbf{X}_{L'_1}^{kpj'} \\ &\quad \times \sum_{\tilde{j}_2, \dots, \tilde{j}_r=0}^{pq-1} \left(\prod_{t=2}^r \omega_p^{k\alpha_t \tilde{j}_t} \omega_q^{\beta'_t(\tilde{j}_t - pj')} x_t^{k\tilde{j}_t} \mathbf{X}_{L'_t}^{k\tilde{j}_t} \right), \end{aligned} \quad (4.44)$$

where β'_t is the sum of the currents β_L 's flowing from the vertex ν_t (with the index j_t) to the vertices $\bar{\nu}_1, \dots, \bar{\nu}_{r'}$ (with j'). For example, in case that the vertex ν_t is attached to three \hat{e}_L 's in E_{12} , say \hat{e}_{L_1} , \hat{e}_{L_2} and \hat{e}_{L_3} , as in Fig, 6, we have $\beta'_t = \beta_{L_1} + \beta_{L_2} + \beta_{L_3}$.

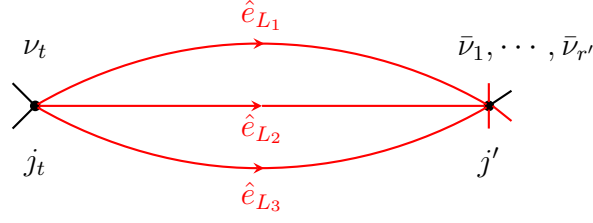


Figure 6: The index j_t is associated to the vertex ν_t , which is attached to the three edges \hat{e}_{L_1} , \hat{e}_{L_2} and \hat{e}_{L_3} in E_{12} . The other ends of the edges are either of the vertices $\bar{\nu}_1, \dots, \bar{\nu}_{r'}$ which are depicted by a single dot, because they are endowed with the common index j' as a result of the computation of Tr_{G_2} . In this case, β'_t in (4.44) is given by $\beta'_t = \beta_{L_1} + \beta_{L_2} + \beta_{L_3}$.

We now define projection operators as

$$\begin{aligned} Q_{1,p} &\equiv \frac{1}{p} \sum_{u=0}^{p-1} \omega_p^{kq\alpha_1 u} x_1^{kqu}, & Q_{1,q} &\equiv \frac{1}{q} \sum_{j'=0}^{q-1} \omega_q^{-pj'(\sum_{t=2}^r \beta'_t)} \mathbf{X}_{L'_1}^{kpj'}, \\ \tilde{Q}_t &\equiv \frac{1}{pq} \sum_{\tilde{j}=0}^{pq-1} \omega_p^{k\alpha_t \tilde{j}} \omega_q^{\beta'_t \tilde{j}} x_t^{k\tilde{j}} \mathbf{X}_{L'_t}^{k\tilde{j}} \end{aligned} \quad (4.45)$$

for $t = 2, \dots, r$, and express (4.44) as

$$(\text{last line of (4.30)}) = k^{-r} Q_{1,p} Q_{1,q} \prod_{t=2}^r \tilde{Q}_t. \quad (4.46)$$

Finally, (4.30) becomes

$$\rho_A^{[\alpha, \beta]} = k^{-r} \left(\prod_{v \in G_1 - \{\nu_1, \dots, \nu_r\}} A_v P_v^{[\alpha_v]} \right) \left(\prod_{e \in G_1} B_e \right) \left(\prod_{L=1}^{B'_1} P_{\hat{e}_L}^{[\beta_L]} \right) Q_{1,p} Q_{1,q} \prod_{t=2}^r \tilde{Q}_t. \quad (4.47)$$

Result of EE It is easy to see that

$$\text{Spec} \left(\rho_A^{[\alpha, \beta]} \right) = \{k^{-r}, 0\}, \quad (4.48)$$

because the RHS of (4.47) is the product of commuting projectors except the factor k^{-r} . It can be directly checked that $\text{Tr} \rho_A^{[\alpha, \beta]} = 1$ holds as it should be from $\text{Tr} \rho^{[\alpha, \beta]} = 1$. This shows that the reduced density matrix has the eigenvalue k^{-r} with the multiplicity k^r .

The bipartite EE is found as

$$S_A^{[\alpha, \beta]} = -\text{Tr} \left(\rho_A^{[\alpha, \beta]} \log_2 \rho_A^{[\alpha, \beta]} \right) = - (k^{-r} \log_2 k^{-r}) \times k^r = (\log_2 k) r. \quad (4.49)$$

This is proportional to r (the ‘area’ of the boundary), which exhibits the area law. The result is independent of the choice of α_v ’s or β_L ’s. There is no constant term, namely the topological EE vanishes.

Comparing to the result for the individual ground state $|\text{GS } s\rangle$ (4.28), we can see that when $\xi = 1$ (i.e., k and p are coprime),

$$S_A^{[\alpha,\beta]} \leq S_{s,A} \quad (4.50)$$

always holds. (4.50) is equivalent to $q^{r-1} \geq 1$, which is valid for any positive integers q and r . When $\xi \neq 1$, (4.50) is equivalent to

$$q \leq \left(\frac{q}{\xi}\right)^r, \quad (4.51)$$

which holds when $q > \xi$ for r large. On the other hand, $S_{s,A}$ is smaller than $S_A^{[\alpha,\beta]}$ when $\xi > q$ for any r .

Note that in the case $S_A^{[\alpha,\beta]} < S_{s,A}$ the basis state maximizing the minus of the topological EE does not minimize the EE due to the contribution from the leading term proportional to r . In [30], since the leading term of the EE is common among the bases of the degenerate ground states, the basis states which maximize the negative of the topological EE are called the *minimum entropy states*. However this does not always hold here, because the basis change affects the leading term as well as the constant term of the EE. For $q > \xi$ this can be seen as a distinguishing feature of our model from the toric code.

5 Excited states

In this section we obtain the first and second excited states of the model. There are anyon-like excitations among them, and their relevance to the obtained topological EE is discussed. Further we discuss the statistics of the obtained anyons for exchange processes that are peculiar to graphs.

Excited states of the models governed by the Hamiltonian in (2.13) appear when at least one of the edge or vertex operators (B_e or A_v) assumes the zero-eigenvalue. Recall that each of these operators has the eigenvalues 0 and 1, since they are projection operators. In particular when some edge operators (vertex operators) take the zero-eigenvalues we will denote them as *edge excitations* (*vertex excitations*). When both edge and vertex operators take zero-eigenvalues we end up with an example of a *combined excitation*. Henceforth we use the phrase, ‘the edge or vertex operators are *excited*’, when they assume the zero-eigenvalues.

In what follows we will show that every edge operator can be excited independently, or in other words all the edge excitations are *isolated*. On the other hand, some of the vertex excitations are isolated and the remaining can only be excited in *pairs*, that is they are *deconfined* and there is no energy cost in moving them around. This can be contrasted with the situation in the abelian quantum double models where all the excitations are deconfined.

In sections 5.1 and 5.2, we discuss excitations on the ground states $|\text{GS } s\rangle$. Excitations on the ground states $|\text{GS}[\alpha, \beta]\rangle$ are similarly constructed.

5.1 Edge excitations

The edge operator (2.9) having the zero-eigenvalue implies that one of its orthogonal complements, $B_e^{[\alpha]}$ in (2.12) with $\alpha \neq 0 \pmod k$, has the eigenvalue 1. To check if a single edge operator on e' is excited we follow the computations of the GSD in section 3.1 to evaluate

$$\text{Tr}_{\mathcal{H}} \left(B_{e'}^{[\alpha]} \prod_{v \in V} A_v \prod_{e \in E - \{e'\}} B_e \right) = p^{|V|} q^{B_1} = \text{GSD} \neq 0, \quad (5.1)$$

which implies the existence of isolated edge excitations for all values of $\alpha \in \{1, 2, \dots, k-1\}$. This exhausts the elementary edge excitations of the theory meaning that a pair of edge excitations has to be composed of two isolated edge excitations.

Excited states $X_e^\beta |\text{GS } s\rangle$: To obtain these isolated edge excitations, let us first pick the state $X_e^\beta |\text{GS } s\rangle$ with $\beta \in \{1, 2, \dots, n-1\}$. The ground state $|\text{GS } s\rangle$ is given by (3.4) and (3.11). Since X_e^k is a local symmetry mapping the ground state to some other ground state, the above state for any β reduces to the form $X_e^\beta |\text{GS } s'\rangle$ with $\beta \in \{1, 2, \dots, k-1\}$. Hence we may consider the case $\beta \in \{1, 2, \dots, k-1\}$ without loss of generality.

From (2.14) we can see that

$$B_e^{(j)} X_e^\beta = \omega_k^{\beta j} X_e^\beta B_e^{(j)} \quad (5.2)$$

and thus

$$B_e X_e^\beta = X_e^\beta B_e^{[\beta]}. \quad (5.3)$$

In addition, since $|s\rangle$ is an eigenstate of B_e with the eigenvalue 1,

$$B_e^{[\alpha]} |s\rangle = 0 \quad \text{for } \alpha \neq 0 \pmod k. \quad (5.4)$$

(5.3) and (5.4) lead to

$$B_e X_e^\beta |\text{GS } s\rangle = 0 \quad \text{for } \beta \in \{1, 2, \dots, k-1\}, \quad (5.5)$$

which implies that $X_e^\beta |\text{GS } s\rangle$ are first excited states with the energy $E_0 + 1$. Here, $E_0 = -|V| - |E|$ is the ground state energy.

We can also apply the operators x_v^β ($\beta \in \{1, 2, \dots, k-1\}$) on the vertices to excite all the edge operators corresponding to the edges attached to the vertex v . As discussed in section 2.3, any power of x_v reduces to the above x_v^β up to the multiplications of the local symmetry operator $(x_v \mathbf{X}_{L_v})^{kq} = x_v^{kq}$. However, x_v^β is not an independent excitation but a collection of the isolated excitations on the edges attached to the vertex v . This follows from

$$x_v^\beta = \left(x_v^\beta \mathbf{X}_{L_v}^\beta \right) \mathbf{X}_{L_v}^{-\beta}, \quad (5.6)$$

where the factor in the parentheses generates a local symmetry. Thus, $x_v^\beta |\text{GS } s\rangle = \mathbf{X}_{L_v}^{-\beta} |\text{GS } s'\rangle$ with $|s'\rangle = \left(x_v^\beta \mathbf{X}_{L_v}^\beta \right) |s\rangle$.

5.2 Vertex excitations

The eigenvalue 0 for the vertex operator in (2.4) corresponds to the eigenvalue 1 for one of the orthogonal vertex operators, $A_v^{[\alpha]}$ in (2.8) with $\alpha \neq 0 \pmod n$. First we look at the possibility for a single vertex operator to be excited, or an isolated vertex excitation, at the vertex v' by computing

$$\text{Tr}_{\mathcal{H}} \left(A_{v'}^{[\alpha]} \prod_{v \in V - \{v'\}} A_v \prod_{e \in E} B_e \right) = \frac{(\text{GSD})}{q} \sum_{b=0}^{q-1} \omega_q^{\alpha b}, \quad (5.7)$$

which does not vanish only when $\alpha = 0 \pmod q$. It implies that $k-1$ isolated vertex excitations exist corresponding to $\alpha \in \{q, 2q, \dots, (k-1)q\}$. As we will see later, the remaining possibilities $\alpha \neq 0 \pmod q$ contribute to deconfined excitations.

Excited states $z_v^\beta |\text{GS } s\rangle$: As in the previous subsection, to create the isolated vertex excitations let us pick the state $z_v^\beta |\text{GS } s\rangle$ with $\beta \in \{1, \dots, m-1\}$. Since z_v^k generates a local symmetry, the cases $\beta \in \{1, \dots, k-1\}$ are candidates for the independent excitations. The relation

$$z_v^\beta A_v^{(j)} = \omega_m^{\beta p j} A_v^{(j)} z_v^\beta \quad (5.8)$$

together with $\omega_m^{\beta pj} = \omega_k^{\beta j} = \omega_n^{\beta qj}$ leads to

$$z_v^\beta A_v = A_v^{[\beta q]} z_v^\beta. \quad (5.9)$$

Then, we have

$$z_v^\beta |\text{GS } s\rangle = \omega_m^{\beta a_v} \sqrt{\mathcal{N}} A_v^{[\beta q]} \left(\prod_{v' \in V - \{v\}} A_{v'} \right) |s\rangle. \quad (5.10)$$

Note that $A_v^{[\beta q]}$ is orthogonal to A_v only when $\beta \neq 0 \pmod k$. Thus, $z_v^\beta |\text{GS } s\rangle$ with $\beta \in \{1, 2, \dots, k-1\}$ are independent isolated vertex excitations with the energy $E_0 + 1$ (first excited states).

Excited states $Z_e^\gamma |\text{GS } s\rangle$: Next we turn our attention to the deconfined vertex excitations that occur in pairs. These are similar to the abelian quantum double models, and hence we first pick the states $Z_e^\gamma |\text{GS } s\rangle$ for $\gamma \in \{1, 2, \dots, n-1\}$. Since $Z_e^{\tilde{n}} = Z_e^{\tilde{k}q}$ generates a local symmetry as mentioned around (2.16), we may consider the cases $\gamma \in \{1, 2, \dots, \tilde{k}q-1\}$. Furthermore,

$$Z_e^{qj} = z_{v_1}^{-pj} [z_{v_1}^{pj} Z_e^{qj} z_{v_2}^{-pj}] z_{v_2}^{pj} = z_{v_1}^{-pj} z_{v_2}^{pj} B_e^{(j)} \quad \text{for } j \in \{1, \dots, k-1\} \quad (5.11)$$

implies that whenever γ is a multiple of q , $Z_e^\gamma |\text{GS } s\rangle$ reduces to a composition of two isolated vertex excitations on v_1 and v_2 , since $B_e^{(j)}$ can be written as a linear combination of the edge operator B_e and its orthogonal complements $B_e^{[\alpha]}$ in (2.12). Thus, we find candidates for independent deconfined vertex excitations as those for $\gamma \in \{1, 2, \dots, q-1\}$.

From (2.14) we obtain for $e \in L_v^\pm$

$$Z_e^\gamma A_v^{(j)} = \omega_n^{\pm \gamma pj} A_v^{(j)} Z_e^\gamma \quad (j \in \mathbb{Z}_n), \quad (5.12)$$

and thus

$$Z_e^\gamma A_v = A_v^{[\pm \gamma p]} Z_e^\gamma. \quad (5.13)$$

Here, $\gcd(p, q) = \gcd(\xi \tilde{p}, q) = 1$ provides $\gcd(\tilde{p}, q) = 1$. This and $\gcd(\tilde{k}, \tilde{p}) = 1$ give $\gcd(\tilde{k}q, \tilde{p}) = 1$, which leads to $\omega_n^{\gamma p} = \omega_{\tilde{k}q}^{\gamma \tilde{p}} \neq 1$ and thus $A_v^{[\pm \gamma p]}$ are orthogonal to A_v for any γ in the above range. For an edge e belonging to $L_{v_1}^-$ and $L_{v_2}^+$ as in Fig. 2, we explicitly see

$$Z_e^\gamma |\text{GS } s\rangle = \omega_q^{p\gamma \sum_{L=1}^{B_1} \delta_{e, \hat{e}_L} b_L} \sqrt{\mathcal{N}} A_{v_1}^{[-\gamma p]} A_{v_2}^{[\gamma p]} \left(\prod_{v' \in V - \{v_1, v_2\}} A_{v'} \right) |s\rangle, \quad (5.14)$$

which indicates that $Z_e^\gamma |\text{GS } s\rangle$ with $\gamma \in \{1, 2, \dots, q-1\}$ are second excited states with the energy $E_0 + 2$. The excitations are paired and occur at the both ends of the edge e , namely the vertices v_1 and v_2 . Now it is clear that among the possibilities of $\alpha \neq 0 \pmod q$ mentioned below (5.7), $q-1$ of them are independent and corresponds to the excitations (5.14).

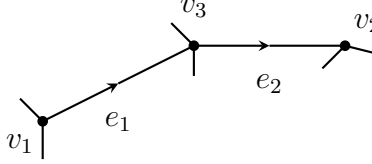


Figure 7: Three vertices v_1 , v_2 and v_3 are connected by two edges e_1 and e_2 such that e_1 is directed from v_1 to v_3 , and e_2 is directed from v_3 to v_2 .

Likewise, for two edges (e_1 and e_2) and three vertices (v_1 , v_2 and v_3), where $e_1 \in L_{v_1}^-, L_{v_3}^+$ and $e_2 \in L_{v_3}^-, L_{v_2}^+$ as in Fig. 7, consecutive two excitations read

$$\begin{aligned} Z_{e_1}^{\gamma_1} Z_{e_2}^{\gamma_2} |\text{GS } s\rangle &= \omega_q^{p \sum_{a=1}^2 \gamma_a \sum_{L=1}^{B_1} \delta_{e_a, \hat{e}_L} b_L} \sqrt{\mathcal{N}} \\ &\times A_{v_1}^{[-\gamma_1 p]} A_{v_3}^{[(\gamma_1 - \gamma_2) p]} A_{v_2}^{[\gamma_2 p]} \left(\prod_{v' \in V - \{v_1, v_2, v_3\}} A_{v'} \right) |s\rangle \end{aligned} \quad (5.15)$$

with $\gamma_1, \gamma_2 \in \{1, 2, \dots, q-1\}$. Note that the relation

$$Z_{e_1}^{\gamma_1} A_{v_3}^{[-\gamma_2 p]} = A_{v_3}^{[(\gamma_1 - \gamma_2) p]} Z_{e_1}^{\gamma_1} \quad (5.16)$$

holds. When $\gamma_1 = \gamma_2$, the excitation at v_3 disappears and (5.15) become second excited states. Based on this observation, we can claim a general statement. Let P be an arbitrary path directed from the vertex v_1 to the vertex v_2 on the graph. For the Wilson line operator along P ,¹⁷

$$Z(P) \equiv \prod_{e \in P} Z_e^{(e|P)}, \quad (5.17)$$

the states $Z(P)^\gamma |\text{GS } s\rangle$ are at the second excited level with the energy $E_0 + 2$ for $\gamma \in \{1, 2, \dots, q-1\}$. The excitations occur at the endpoints of P , v_1 and v_2 .

5.3 Case of $m = 4, n = 6$

For illustrative purposes of the peculiarities of the excited states, we concretely present the case of $m = 4$ and $n = 6$, i.e., $k = p = 2$ and $q = 3$. In this case there are six mutually orthogonal

¹⁷ $(e|P)$ is a sign factor defined similarly to $(e|C)$ at (2.17).

vertex operators, $A_v^{[\alpha]}$, $\alpha \in \{0, 1, \dots, 5\}$, and two mutually orthogonal edge operators, $B_e^{[\alpha]}$, $\alpha \in \{0, 1\}$. These operators are given in (2.8) and (2.12) respectively and for clarity we write their full expressions here.

$$\begin{aligned}
A_v^{[0]} &= \frac{1}{6} [1_v 1_{L_v} + x_v^2 \mathbf{X}_{L_v}^2 + 1_v \mathbf{X}_{L_v}^4 + x_v^2 1_{L_v} + 1_v \mathbf{X}_{L_v}^2 + x_v^2 \mathbf{X}_{L_v}^4], \\
A_v^{[1]} &= \frac{1}{6} [1_v 1_{L_v} + \omega_6 x_v^2 \mathbf{X}_{L_v}^2 + \omega_6^2 1_v \mathbf{X}_{L_v}^4 + \omega_6^3 x_v^2 1_{L_v} + \omega_6^4 \mathbf{X}_{L_v}^2 + \omega_6^5 x_v^2 \mathbf{X}_{L_v}^4], \\
A_v^{[2]} &= \frac{1}{6} [1_v 1_{L_v} + \omega_3 x_v^2 \mathbf{X}_{L_v}^2 + \omega_3^2 1_v \mathbf{X}_{L_v}^4 + x_v^2 1_{L_v} + \omega_3 \mathbf{X}_{L_v}^2 + \omega_3^2 x_v^2 \mathbf{X}_{L_v}^4], \\
A_v^{[3]} &= \frac{1}{6} [1_v 1_{L_v} - x_v^2 \mathbf{X}_{L_v}^2 + 1_v \mathbf{X}_{L_v}^4 - x_v^2 1_{L_v} + 1_v \mathbf{X}_{L_v}^2 - x_v^2 \mathbf{X}_{L_v}^4], \\
A_v^{[4]} &= \frac{1}{6} [1_v 1_{L_v} + \omega_3^2 x_v^2 \mathbf{X}_{L_v}^2 + \omega_3 1_v \mathbf{X}_{L_v}^4 + x_v^2 1_{L_v} + \omega_3^2 \mathbf{X}_{L_v}^2 + \omega_3 x_v^2 \mathbf{X}_{L_v}^4], \\
A_v^{[5]} &= \frac{1}{6} [1_v 1_{L_v} + \omega_6^5 x_v^2 \mathbf{X}_{L_v}^2 + \omega_6^4 1_v \mathbf{X}_{L_v}^4 + \omega_6^3 x_v^2 1_{L_v} + \omega_6^2 \mathbf{X}_{L_v}^2 + \omega_6 x_v^2 \mathbf{X}_{L_v}^4],
\end{aligned}$$

and

$$\begin{aligned}
B_e^{[0]} &= \frac{1}{2} [1_{v_1} 1_e 1_{v_2} + z_{v_1}^2 Z_e^3 z_{v_2}^2], \\
B_e^{[1]} &= \frac{1}{2} [1_{v_1} 1_e 1_{v_2} - z_{v_1}^2 Z_e^3 z_{v_2}^2].
\end{aligned}$$

Here, $\omega_6 = e^{\frac{2\pi i}{6}}$, $\omega_3 = e^{\frac{2\pi i}{3}}$, $x_v^4 = z_v^4 = 1_v$ and $X_e^6 = Z_e^6 = 1_e$. While the ground states are the +1 eigenstates of $A_v^{[0]}$ and $B_e^{[0]}$, the excited states are +1 eigenstates of the remaining orthogonal operators, as discussed in sections 5.1 and 5.2. We will exhaust them using the results of sections 5.1 and 5.2.

The first excited states are given by $X_e|\text{GS } s\rangle$ and $z_v|\text{GS } s\rangle$ for any $e \in E$ and $v \in V$, which are isolated (immobile) and appear when $k \neq 1$ in general. They are the isolated edge and vertex excitations and are easily seen as the +1 eigenstates of the operators, $B_e^{[1]}$ and $A_v^{[3]}$, respectively. The second excited states are given by $Z(P)|\text{GS } s\rangle$ and $Z(P)^2|\text{GS } s\rangle$ with $Z(P)$ being (5.17) for any open path on the graph G , which are deconfined (mobile) and appear when $q \neq 1$ in general.

The operators $Z(P)$ and $Z(P)^2$ create vertex excitations at the endpoints of the path P , which are the +1 eigenstates of the vertex operators, $A_v^{[2]}$ and $A_v^{[4]}$. Finally appending the operators z_v at the end points of the path operators, $Z(P)$ and $Z(P)^2$ we create the +1 eigenstates of the operators, $A_v^{[1]}$ and $A_v^{[5]}$. Interestingly, these combined excitations are also at the second excited level.¹⁸

¹⁸We did not considered such combined excitations in section 5.2 because the analysis seems to be complicated for general m and n .

Note that there are no deconfined excited states created by X_e . This realizes the exchange phases of ‘anyons’ which are not exactly the same as what appear in the toric code or the two-dimensional quantum double models of Kitaev (see the following subsections).

5.4 Anyon-like excitations and topological EE

In this section we discuss anyon-like excitations and their relevance to the topological EE computed in sections 4.1 and 4.2.

Let us first recall the toric code model [4]. The toric code model is defined on the square lattice¹⁹ with the Pauli spin operators, \bar{X}_e and \bar{Z}_e , acting on each link.²⁰ The Hamiltonian consists of two kinds of interaction terms – the star term A_v consisting of \bar{X}_e ’s and the plaquette term B_p consisting of \bar{Z}_e ’s. The former energetically imposes the Gauss law constraints, and the latter gives a standard gauge kinetic term on the lattice. It is analogous to the \mathbb{Z}_2 lattice gauge theory. There are two kinds of deconfined excitations. One is ‘electric excitations’ which are constructed by Wilson line operators of \bar{Z}_e acting on the ground states. Associated to a path on the (original) lattice, the corresponding Wilson line operator is defined by the product of \bar{Z}_e ’s along the path. The excitations occur at the endpoints of the path, which can be interpreted as electric charges. The other is ‘magnetic excitations’ constructed by acting ’t Hooft line operators on the ground states. Associated to a path on the dual lattice, the corresponding ’t Hooft line operator is defined by the product of \bar{X}_e ’s on the edges e intersecting with the path. The excitations appear at the endpoints of the path, which can be interpreted as magnetic fluxes. When an electric charge moves around a magnetic flux (and vice versa), an anyon phase appears due to the Aharonov-Bohm effect. See Fig. 8 for an example of ’t Hooft and Wilson line operators.

Clearly the electric excitations correspond to the Wilson line operators $Z(P)^\gamma$ ($\gamma = 1, 2, \dots, q - 1$) acting on the ground states in our case. However, there seems to be no counterpart to the magnetic excitations in excitations discussed in sections 5.1 and 5.2. We see that the \mathbb{Z}_q magnetic fluxes pb_L ’s on the ground states $|\text{GS}s\rangle$ play an analogous role to the magnetic excitations, except the point that the magnetic fluxes do not cost any energy, or they are condensed into the ground state. In our case, since the plaquette terms of Z_e ’s are absent in the Hamiltonian (2.13), the ground states can accommodate the zero-energy

¹⁹The toric code models are well-defined on any triangulation of the two dimensional space, and the square lattice is usually chosen for simplicity.

²⁰We put the bar to the operators of the toric code model in order to distinguish the operators in our model.

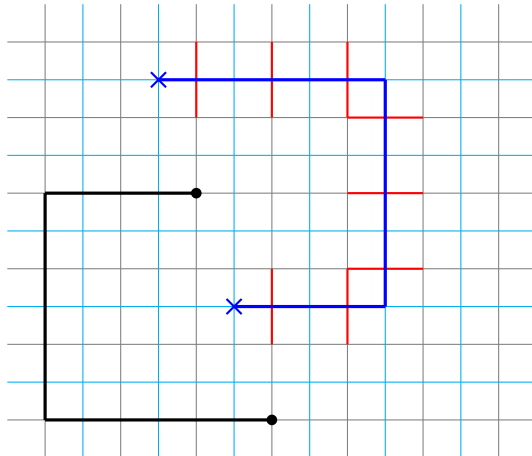


Figure 8: An example of 't Hooft and Wilson line operators in the toric code model on the square lattice. For the original lattice drawn in the gray lines, the dual lattice is drawn in the light blue lines. The blue line represents a path on the dual lattice, and its associated 't Hooft line operator is given by the product of \bar{X}_e 's on the red edges. The blue crosses represent the ends of the 't Hooft line, at which magnetic excitations occur. The black line is a path on the original lattice. The product of \bar{Z}_e 's along the path gives the associated Wilson line. Electric excitations appear at the endpoints of the path (the black dots).

magnetic fluxes.²¹ From (3.16), after one of the endpoints of the Wilson line circulates along the closed path C_L , it acquires the Aharonov-Bohm phase²²

$$\omega_q^{p\gamma b_L (\hat{e}_L|C_L)}. \quad (5.18)$$

Since a general closed path on the graph is a linear combination of C_L 's with the coefficients ± 1 , the phase appearing after moving along the general path is given by the product of the phases for each C_L . In the phase (5.18), γ and b_L are \mathbb{Z}_q -valued (including the trivial case), which leads to the total quantum dimension $D = \sqrt{q^2} = q$. This accounts for the topological EE term obtained in section 4.1.

On the other hand, the ground states $|\text{GS}[\alpha, \beta]\rangle$ have the \mathbb{Z}_q electric flux $\beta_L(\hat{e}_L|C_L)$ along

²¹Interestingly, adding the plaquette terms of Z_e^q 's rather than Z_e 's to the Hamiltonian does not alter the ground states.

²²A similar phenomenon is observed in *topological flux phases* in the *string net models* [39]. Although the string net models normally allow ground states with zero flux, the topological flux phases are realized by modifying the Hamiltonians so that nonzero flux states are energetically favored [40].

C_L as shown in section 3.3. β_L corresponds to γ in the above. Thus the same process acquiring the anyon phase (5.18) occurs by inserting the *local operator* $X_{\hat{e}_L}^{-pbk(\hat{e}_L|C_L)}$ ($b \in \mathbb{Z}_q$). As is seen from (3.24),

$$X_{\hat{e}_L}^{-pbk(\hat{e}_L|C_L)}|\text{GS}[\alpha, \beta]\rangle = \omega_q^{pb_L\beta_L(\hat{e}_L|C_L)}|\text{GS}[\alpha, \beta]\rangle. \quad (5.19)$$

This operator is local and does not contribute to the topological EE, which explains the reason why the topological EE vanishes for $|\text{GS}[\alpha, \beta]\rangle$ in the result (4.49).

5.5 Exchange statistics on graphs

Before closing this section, we mention about connections to the analysis in [16–18] to identify exchange statistics that are peculiar to graphs. There, quantum particles sit on vertices of graphs, and it is investigated which phases can appear for various patterns of the exchange of the particles. The setting is different from the case of the abelian toric code models, in which an anyon phase appears only when an electric excitation at a vertex of the (original) lattice moves around a magnetic one at a vertex of the *dual lattice* and vice versa. When an electric excitation moves around another electric one, no phase appears.

Similarly, in our case, movable excitations at vertices are only of the electric type, and their exchange as in Fig. 9 does not provide a nontrivial phase. However, in case that the ground state $|\text{GS } s\rangle$ has magnetic flux penetrating the region enclosed by the loop $C : v_1 \rightarrow v_2 \rightarrow v_3 \rightarrow v_4 \rightarrow v_1$, the Aharonov-Bohm phase appears as already mentioned. Interestingly, even when the ground state does not have the magnetic flux, and instead an isolated excitation X_e^β ($\beta \in \{1, \dots, k-1\}$) exists on some edge e on the loop, a nontrivial phase appears as

$$Z(C)^\gamma X_e^\beta |\text{GS } s\rangle = \omega_n^{\beta\gamma(e|C)} X_e^\beta Z(C)^\gamma |\text{GS } s\rangle = \omega_n^{\beta\gamma(e|C)} X_e^\beta |\text{GS } s\rangle, \quad (5.20)$$

where $\gamma \in \{1, \dots, q-1\}$, and the last equality comes from (3.16) with $b_L = 0$ (no magnetic flux). This can be thought of as a generalization of the Aharnov-Bohm effect in the presence of the 0-holonomy operator or the edge operator.

In addition, the exchange on a T- (or Y-) junction is considered in [16–18], where two particles at the vertices (v_3, v_2) move as $(v_3, v_2) \rightarrow (v_3, v_4) \rightarrow (v_2, v_4) \rightarrow (v_1, v_4) \rightarrow (v_1, v_2) \rightarrow (v_1, v_3) \rightarrow (v_2, v_3)$ in Figs. 10 and 11. In our case no phase appears in the process as seen below.

Let us consider two deconfined excitations of strings $Z(P_1)^{\gamma_1}$ and $Z(P_2)^{\gamma_2}$ ($\gamma_1, \gamma_2 \in \{1, \dots, q-1\}$) on any fixed state $|\psi\rangle$. Suppose the T-(or Y-) junction is a part of the graph and the red

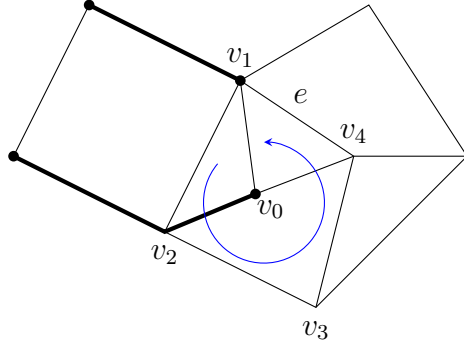


Figure 9: Two Wilson lines on a graph. The thick lines denote the Wilson lines. The orientations are suppressed. When the excitation at the vertex v_1 move around the excitation at v_0 along the loop $C : v_1 \rightarrow v_2 \rightarrow v_3 \rightarrow v_4 \rightarrow v_1$ (as the blue arrow indicates), there appears no anyon phase because they are both electric excitations. Interestingly, if there is an isolated excitation on some edge e on the loop C , the electric excitation moves along C on $X_e^\beta |GS s\rangle$ ($\beta = \{1, \dots, k-1\}$) provides a phase.

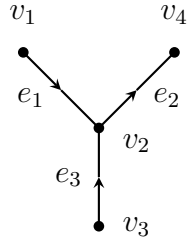


Figure 10: A graph of a T- (or Y-) junction.

and blue dots in Fig. 11 are endpoints of $Z(P_1)^{\gamma_1}$ and $Z(P_2)^{\gamma_2}$, respectively. When $e_3 \in P_1$,²³ the initial state is written as

$$|\psi_i\rangle = Z_{e_3}^{\gamma_1} \cdots |\psi\rangle, \quad (5.21)$$

where (\cdots) expresses the strings outside the T-(Y-) junction and does not change in the process (see Fig. 12). We trace the path of each of the strings in the exchange process. The endpoint of the string $Z(P_1)^{\gamma_1}$ (the red dot) moves as $v_2 \rightarrow v_4 \rightarrow v_2 \rightarrow v_3$ which gives the additional contribution to the string

$$Z_{e_3}^{-\gamma_1} Z_{e_2}^{-\gamma_1} Z_{e_2}^{\gamma_1} = Z_{e_3}^{-\gamma_1}, \quad (5.22)$$

whereas the endpoint of the string $Z(P_2)^{\gamma_2}$ (the blue dot) moves as $v_3 \rightarrow v_2 \rightarrow v_1 \rightarrow v_2$ which

²³We can similarly show for other configurations of the path.

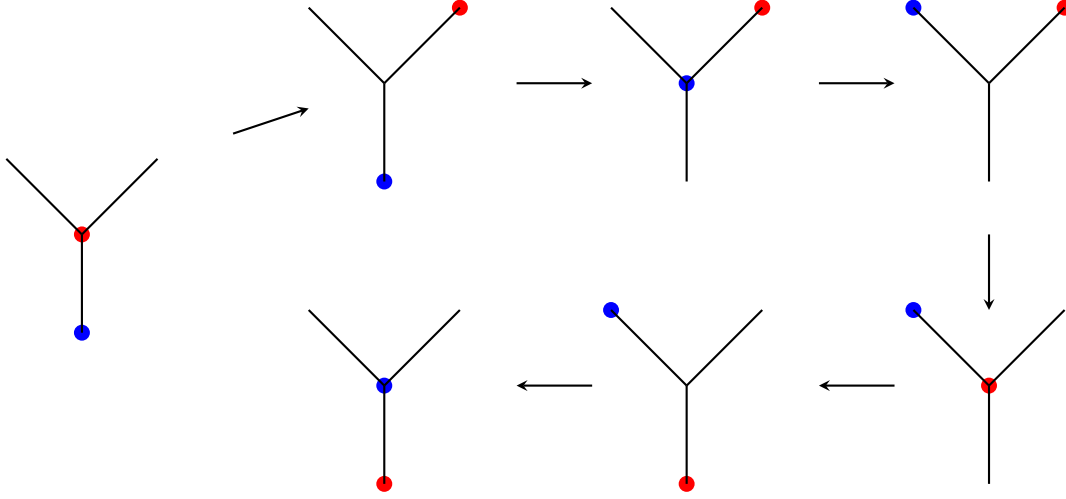


Figure 11: The exchange process of two particles (the red and blue dots) in a T-(Y-) junction of the graph. For simplicity the orientations and other vertices are suppressed.

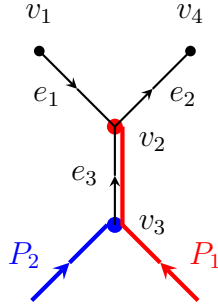


Figure 12: An initial configuration of the strings $Z(P_1)^{\gamma_1}$ (red line) and $Z(P_2)^{\gamma_2}$ (blue line).

yields

$$Z_{e_1}^{\gamma_2} Z_{e_1}^{-\gamma_2} Z_{e_3}^{\gamma_2} = Z_{e_3}^{\gamma_2}. \quad (5.23)$$

Thus, $Z_{e_3}^{-\gamma_1+\gamma_2}$ is obtained in total. Including this, the final state becomes

$$|\psi_f\rangle = Z_{e_3}^{-\gamma_1+\gamma_2} |\psi_i\rangle = Z_{e_3}^{\gamma_2} \cdots |\psi\rangle. \quad (5.24)$$

(5.24) is the same as (5.21) after γ_2 is replaced by γ_1 , which realizes the exchange without a phase. Note that this holds for any state $|\psi\rangle$ ²⁴.

²⁴As a remark we would like to add that it is possible to obtain exchange phases in this process if we move the deconfined vertex excitations with $Z_e^{q-\gamma}$ instead of $Z_e^{-\gamma}$. This is allowed as $\gamma \in \{1, 2, \dots, q-1\}$. However this exchange process is not adiabatic as Z_e^q (See (5.11)) creates extra vertex excitations changing the energy

6 Discussion

6.1 Summary

In this paper we have initiated a detailed study of abelian gauge theories on graphs that host quantum phases not classified as phases of spontaneous symmetry breaking with local order parameters. In general the models realize such quantum phases with a mixture of topological and extensive aspects.²⁵ They possess features that are reminiscent of the two-dimensional quantum double models of Kitaev [4], with some subtle differences in their properties, notably in the GSD and in the nature of the anyonic excitations.

In some cases occurring for specific families of m and n values, our result reads:

- When $p = 1$, n is an integer multiple of m : $n = mq$. We obtain the purely topological case in which the GSD reduces to q^{B_1} . The EE for the ground states, $|\text{GS } s\rangle$, includes the constant term (topological EE) as $-\gamma = -\log_2 q$, accounted for by the anyons in the model.
- When $q = 1$, m is an integer multiple of n : $m = np$. The GSD is extensive as seen by the expression $p^{|V|}$. For the ground states $|\text{GS } s\rangle$, the topological EE vanishes.
- When $m = n$, there is a unique ground state obeying the area law for the EE. It is also interesting to note that the Hamiltonian for $m = n = 2$ is unitarily equivalent to the *cluster state Hamiltonians* representing a $\mathbb{Z}_2 \times \mathbb{Z}_2$ *symmetry protected topological* (SPT) phase [41], when the graph forms either an open or closed chain.
- When $k = 1$, $m = p$ and $n = q$ are co-prime to each other. We do not have valid homomorphisms, $\partial^{[l]}$ between \mathbb{Z}_n and \mathbb{Z}_m except for the trivial homomorphism. In this case, the edge operators become trivial ($B_e = 1$), and the vertex operators reduce to

of the state during the exchange process. The phase, upon exchanging the deconfined vertex excitations in the background of three isolated edge excitations created by $X_{e_1}^{\beta_1}$, $X_{e_2}^{\beta_2}$ and $X_{e_3}^{\beta_3}$ is, $\omega_n^{q\beta_1 + q\beta_2 + 2q\beta_3}$.

²⁵According to Theorem IV.6 in [23], the GSD is given by

$$\text{GSD} = \prod_n |H^n(C, H_n(G))| = \underbrace{|\text{Hom}(H_0(C), H_0(G))|}_{p^{|V|}} \underbrace{|\text{Hom}(H_1(C), H_1(G))|}_{p^{|E| - |V| + 1}}$$

since the Ext and Tor functors are null. This implies that the extensive part of the GSD, $p^{|V|}$, can also be regarded as a topological contribution from the mathematical perspective. However, we should remark that each of the ground states contributing to the extensive part is fragile under local perturbations, as mentioned in the last paragraph of this section, defying the physicist's definition of topological phases.

$A_v = \frac{1}{q} \sum_{j=0}^{q-1} 1_v \mathbf{X}_{L_v}^{pj}$ which impose the Gauss law constraints of the pure gauge theory. Although only the operators X_e appear in the Hamiltonian, the result for the GSD, $p^{|V|} q^{B_1}$ is still valid, and the EE for the ground states $|\text{GS } s\rangle$ includes the global constant term $-\gamma = -\log_2 q$. All the excitations are deconfined and given by the Wilson line operators, which constitute anyon-like excitations in the interplay with the magnetic fluxes in the ground states.

6.2 Outlook

We present some directions for further study:

- The toric code model can be extended to a lattice discretizing surfaces with boundary [42, 43]. It is worth considering a similar extension in the models on graphs presented here. In general, it seems nontrivial to divide a graph into bulk and boundary parts. Tree graphs and finite regular lattices are examples in which such a division is possible. In the tree graph, vertices with valency 1 are identified as boundaries. In the finite square lattice, vertices with valency 2 or 3 and edges connecting them form the boundary. It is interesting to find some other class of graphs such that the division is possible. If the models are defined on these graphs with appropriate modifications to the Hamiltonian at the boundary, we expect to see the appearance of *edge states* similar to what happens in the SPT case. This will lead to an extra degeneracy in the number of ground states in addition to the topological and the extensive degeneracy already present. The *tree graph* is a special case where we do not expect any topological degeneracy as $B_1 = 0$ in this case. The interesting thing to note is that these edge states may not result from a fractionalization of a *global symmetry* as it happens in the SPT case [44].
- Generalizations of these models to finite non-abelian groups are possible along the lines presented in [25]. These are however much harder to analyze. It is also natural to see if these models can be generalized to other algebras much like the quantum double models of Kitaev. With the machinery developed in [25] this might be possible as well.
- Locally the vertex and plaquette operators of the quantum double models satisfy the relations of a *quasitriangular Hopf algebra* [7]. In fact Drinfeld's quantum double construction is tailored to construct such algebras that have the R -matrix satisfying the Yang-Baxters equation encoded in them. This gives rise to the anyon excitations which are the IRR's of this algebra [6]. It would be very interesting to study the way in which

this algebra is modified for the operators presented here. Naturally we may expect them to have some generator that can realize the relations of the graph braid groups.

- The result obtained here is valid for the same model defined on lattices in arbitrary dimensions, because graphs includes lattices in any dimensions. It is expected that these results apply to a broad class of lattice models.
- We have seen that the GSD of these models are a mixture of a topological invariant (first Betti number) and an extensive quantity depending on the lattice size. Moreover apart from the anyonic excitations that account for the topological EE, there are other *immobile* excitations that cannot be moved around the graph. These features are very similar to those present in the *fracton phases of matter* as discussed in [45–47]. We hope to explore more of this connection.
- These systems can also be viewed as stabiliser codes and it is natural to look for an application in quantum computation. However for the case when $q \neq 1$ there are weight 1 symmetries implying that single qubit operations move us within the logical space making them undetectable. Thus direct application of our models to quantum error correction seems to be restrictive to the case $p = 1$. For $p \neq 1$, the $p^{|V|}$ ground states $|\text{GS}[\alpha, \beta]\rangle$ with fixed β_L 's are flipped to one another by local perturbations as seen in (3.26). From (3.27), the $p = 1$ case seems interesting especially when the lengths of all the closed paths C_L grow as the size of the graph G , $|V|$ or $|E|$, increases. Then, the ground states $|\text{GS}[-, \beta]\rangle$ (there is no α parameter when $p = 1$) are expected to be robust against local perturbations and useful for error correcting purposes. We present such an example in Fig. 13. The size of the graph, $|E|$ or $|V|$, grows as N increases. Then, both the size of the holes and the number of holes also scale. The logarithm of the GSD is subextensive: $\log_2(\text{GSD}) = O(N^2) = O(|V|^{2/3}) = O(|E|^{2/3})$. From the quantum computation perspective, $|\text{GS}[-, \beta]\rangle$'s are logical qudits. Starting from any state of $|\text{GS}[-, \beta]\rangle$'s, we can exhaust all the logical qudits by successively acting $Z(C_L)$'s as seen in (3.27). The logical operations grow with the system size just as in the case of surface codes. The example seems to realize robustness under local perturbations and the growth of the number of logical qudits as N increases.
- As a final remark we note that it is possible to go beyond the chain complex/higher gauge formulation presented in [23, 24] with the following example :

$$A_v = \frac{1}{m} \sum_{j=0}^{m-1} x_v^{qj} \mathbf{X}_{L_v}^{qj}, \quad B_e = \frac{1}{k} \sum_{j=0}^{k-1} z_{v_1}^{pj} Z_e^{qj} z_{v_2}^{-pj}. \quad (6.1)$$

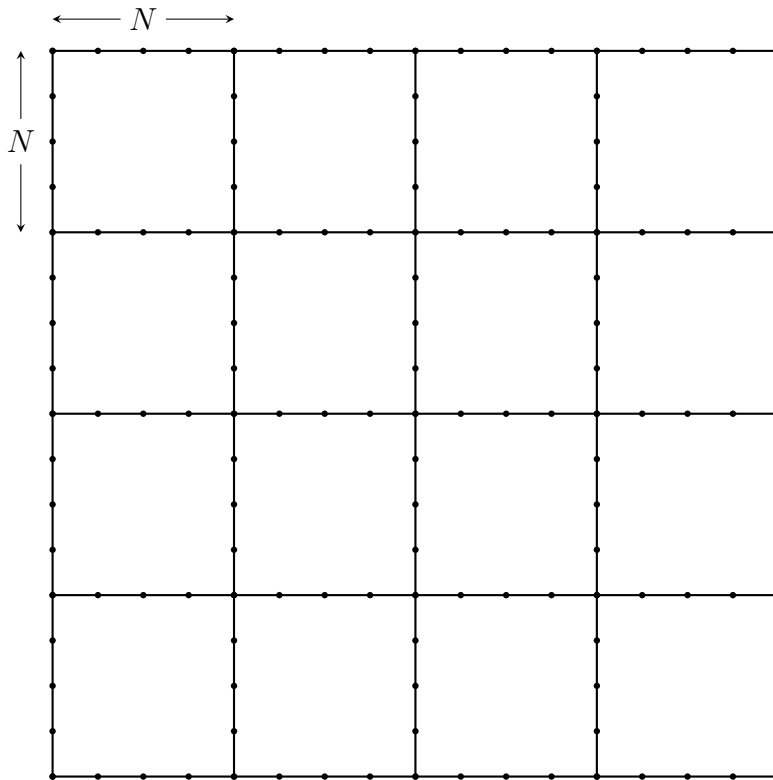


Figure 13: A graph whose shape is a coarse net. The orientations of the edges are suppressed. The size of each hole of the net is $N \times N$, and the number of the holes is $B_1 = N^2$. $|E| = 2N^3 + 2N^2$ and $|V| = 2N^3 + N^2 + 1$. The case $N = 4$ is depicted.

This model can be thought of as the one where the 0-gauge fields on the vertices act on the 1-gauge fields on the edges,

$$\tilde{\partial} : \mathbb{Z}_m \rightarrow \mathbb{Z}_n; \quad \tilde{\partial}(j) = qj, \quad (6.2)$$

which is a valid homomorphism as $\tilde{\partial}(m) = qm = pn \equiv 0 \pmod{n}$. It is opposite to the direction of the homomorphism ∂ . This model has a ground state degeneracy given by

$$\text{GSD} = q^{|E|} \eta, \quad (6.3)$$

with $\eta = \text{gcd}(q, m)$. We hope to analyze these directions in the future.

Acknowledgements

FS is supported by the Institute for Basic Science in Korea (IBS-R018-D1).

A Analogy to quantum field theory with $U(1)$ gauge field and a matter field

To gain an intuitive understanding of our model, we consider an analogy to quantum field theory with $U(1)$ gauge field \vec{A} and a complex scalar field ϕ for charged matter. \vec{A} means space components of the gauge field, and the time component A_0 is supposed to be fixed at $A_0 = 0$.

The second term in the Hamiltonian (2.13), $-\sum_{e \in E} B_e$, can be regarded as the kinetic term of the matter field $|\vec{D}\phi|^2$, where \vec{D} denotes the covariant derivative associated to the gauge field. Then, we can interpret Z_e and z_v as (the exponential of) the gauge field \vec{A} and the matter field ϕ , respectively. (2.17) corresponds to the Wilson loop, and $|h_v\rangle \in \mathcal{H}_v$ ($|i_e\rangle \in \mathcal{H}_e$) correspond to the eigenstate of the matter field ϕ (the gauge field \vec{A}).

As mentioned in section 2.1, the first term in (2.13), $-\sum_{v \in V} A_v$, imposes the gauge invariance energetically. Namely, the gauge symmetry is preserved on the eigenstates of A_v with the eigenvalue 1 for all $v \in V$. A_v is analogous to an operator imposing the Gauss law constraint $\text{div } \vec{E} - \rho_{\text{matter}} = 0$ (\vec{E} and ρ_{matter} stand for the electric field and the matter charge density, respectively). We can interpret X_e and x_v as the electric field (the conjugate momentum of the gauge field) and the conjugate momentum π of the matter field.

The Hamiltonian (2.13) does not possess the plaquette terms of Z_e which corresponds to the gauge kinetic terms $\vec{E}^2 + \vec{B}^2$ with $\vec{B} \equiv \text{rot } \vec{A}$ in the gauge field theory.

Note that the Wilson loop $\exp\left(i \int_C d\vec{x} \cdot \vec{A}\right)$ along a loop C in the space creates the unit electric flux along the loop, which is seen from its canonical commutation relation with \vec{E} : $[A_i(t, \vec{x}), E_j(t, \vec{x}')] = i\delta_{ij}\delta(\vec{x} - \vec{x}')$.

B $U(1)$ gauge theory on a circle

In this appendix we briefly review $U(1)$ gauge theory defined on a circle and the property of its vacuum, in order to help understanding the ground states in sections 3.2 and 3.3.

For a mathematically well-defined treatment, we also impose the periodic boundary conditions in the time direction $x^0 = t \in [0, T]$ as well as the space direction $x^1 = x \in [0, L]$. After final results are obtained, we can send T to infinity. In gauge theory it is sufficient that gauge

fields are periodic modulo gauge transformations. In general, gauge fields $A_\mu(t, x)$ ($\mu = 0, 1$) satisfy

$$A_\mu(T, x) = A_\mu(0, x) + ih(x)\partial_\mu h(x)^{-1}, \quad A_\mu(t, L) = A_\mu(t, 0) + ig(t)\partial_\mu g(t)^{-1}, \quad (\text{B.1})$$

where $h(x), g(t) \in U(1)$ are transition functions at $t = T$ and $x = L$, respectively. In order to obtain topologically nontrivial configurations (nontrivial $U(1)$ bundles over the 2-torus), we take

$$h(x) = \exp\left(\frac{2\pi i}{L}n_x x\right), \quad g(t) = \exp\left(\frac{2\pi i}{T}n_t t\right) \quad (n_x, n_t \in \mathbb{Z}) \quad (\text{B.2})$$

as an example. Those with nontrivial n_x and n_t cannot be obtained by continuous deformations from the identity: $h(x) = 1$ and $g(t) = 1$. As discussed in [48], we can undo one of the twists, say $g(t)$, using a gauge transformation $\Omega(t, x)$ such that $\Omega(t, 0) = 1$ and $\Omega(t, L) = g(t)$. For example, we take

$$\Omega(t, x) = \exp\left(\frac{2\pi i}{TL}n_t tx\right), \quad (\text{B.3})$$

and then obtain

$$A_\mu(T, x) = A_\mu(0, x) + \delta_{\mu,1} \frac{2\pi\nu}{L}, \quad A_\mu(t, L) = A_\mu(t, 0) \quad (\text{B.4})$$

with $\nu = n_x - n_t$.

In the boundary conditions (B.4), we can take the $A_0 = 0$ gauge. Then, topologically nontrivial gauge transformations labelled by an integer $\nu \in \mathbb{Z}$ are given by $h_\nu(x) = \exp\left(\frac{2\pi i}{L}\nu x\right)$ times topologically trivial gauge transformations. The topologically trivial gauge transformations are connected to the identity by continuous deformations. The configuration space of the gauge field A_1 is also divided into the sectors. Namely, configurations satisfying

$$A_1(T, x) = A_1(0, x) + \frac{2\pi\nu}{L} \quad (\text{B.5})$$

belong to the sector ν . Correspondingly the Hilbert space is classified by the topological number ν . Given an initial state (at $t = 0$) with the topological number ν_0 , time evolution of the system under the condition (B.5) leads to a final state (at $t = T$) with the topological number $\nu + \nu_0$. The vacuum with the topological number ν , $|\Omega_\nu\rangle$ ($\nu \in \mathbb{Z}$), is changed to the one with different ν by topologically nontrivial gauge transformations. However, the θ -vacuum defined by

$$|\theta\rangle \equiv \sum_{\nu \in \mathbb{Z}} e^{i\nu\theta} |\Omega_\nu\rangle \quad (\text{B.6})$$

becomes an eigenstate for any gauge transformation.

From (B.5) it can be seen that ν is equal to the first Chern number:

$$c_1 \equiv \frac{1}{2\pi} \int_0^T dt \int_0^L dx F_{01} = \frac{1}{2\pi} \int_0^T dt \int_0^L dx \partial_0 A_1 = \frac{1}{2\pi} \int_0^L dx [A_1(T, x) - A_1(0, x)] = \nu. \quad (\text{B.7})$$

This formula indicates that the vacuum in the nontrivial topological sector $|\Omega_\nu\rangle$ has a non-trivial background field strength F_{01} . Suppose we can take a simply connected domain surrounded by the circle $[0, L]$. Magnetic flux penetrating the domain can be expressed as $\Phi(t) = \int_0^L dx A_1(t, x)$. Then (B.7) immediately gives

$$\Phi(T) - \Phi(0) = 2\pi\nu, \quad (\text{B.8})$$

which means that the twist (B.5) provides the magnetic flux $2\pi\nu$.

For a system on a graph as we are discussing in the text, we can consider a subsystem on each closed path C_L analogously to the $U(1)$ theory on a circle here, at least regarding the topological structure of the ground states.

C Short review of graph homology

Algebraic topology helps distinguish topological spaces systematically. The fundamental group and higher homotopy groups classify topological spaces by characterizing the *holes* of different dimensions in these spaces but they quickly become hard to interpret as we increase the dimension of the topological space. A commutative alternative to homotopy is given by *homology* theory which we are concerned with.

If X is a topological space we can construct a sequence of groups, $H_n(X)$ for $n = 0, 1, 2, \dots$, termed as the homology groups. These are commutative and their rank measures the number of n dimensional holes in X . We will illustrate these groups with the simplest example of X , a graph. Consider the graph shown in Fig. 14.

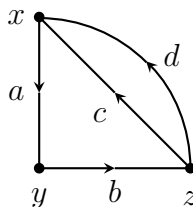


Figure 14: A directed graph, X with three vertices, $\{x, y, z\}$ and four edges, $\{a, b, c, d\}$.

This graph is made up of three vertices x, y, z and four edges a, b, c, d . The edges are directed as shown in Fig. 14. The vertices are also called *0-simplices* and the edges, *1-simplices*. Together the graph X is a *simplicial complex*. Naturally higher dimensional surfaces correspond to higher simplices but here we restrict ourselves to 0- and 1-dimensional simplices as we are interested in graphs.

The set of vertices is denoted by C_0 and is the free abelian group generated by the vertices x, y, z . A general element of C_0 is $\alpha x + \beta y + \gamma z$ with the coefficients α, β, γ being numbers in some field which we take to be the integers, \mathbb{Z} . Likewise, the set of edges is denoted by C_1 and is the free abelian group generated by a, b, c, d . In the literature the elements of C_0 and C_1 are called zero- and one-dimensional chains, respectively.

We now consider a group homomorphism,

$$C_1 \xrightarrow{\partial_1} C_0,$$

which is called the *boundary map*. As the name implies it maps the edge in C_1 to its boundary in C_0 . For the case of the graph X in Fig. 14 we obtain

$$\partial_1(a) = y - x, \quad \partial_1(b) = z - y, \quad \partial_1(c) = x - z, \quad \partial_1(d) = x - z. \quad (\text{C.1})$$

Clearly the 0-chains $y - x, z - y$, etc are the *boundaries* of the 1-chains or edges. We can now think of special 1-chains called *cycles* whose boundary is null. For the graph X in Fig. 14 we obtain three cycles, $a + b + c, a + b + d$ and $c - d$, each of whose boundaries evaluate to 0. A crucial property of the boundary map,

$$\partial^2 = 0, \quad (\text{C.2})$$

can be verified by evaluating ∂_1^2 in X .

Consider the *short exact sequence*

$$0 \xrightarrow{\partial_2} C_1 \xrightarrow{\partial_1} C_0 \xrightarrow{\partial_0} 0. \quad (\text{C.3})$$

The homology groups H_n are defined as

$$H_n(X) = Z_n/B_n, \quad (\text{C.4})$$

where Z_n are the group of cycles and B_n are the group of boundaries. More precisely $Z_n = \text{Ker}(\partial_n)$ and $B_n = \text{Im}(\partial_{n+1})$. The quotient Z_n/B_n collects n -chain cycles that are not

boundaries of $n + 1$ -chains. Thus it is the group generated by the independent n -dimensional cycles or holes.

Thus for the graph X in Fig. 14 we can compute $H_1 = \text{Ker}(\partial_1)/\text{Im}(\partial_2)$. $\text{Ker}(\partial_1) = \mathbb{Z} \oplus \mathbb{Z}$ is generated by $a + b + c$ and $a + b + d$ (two of the obtained three cycles are linearly independent), and $\text{Im}(\partial_2) = 0$ as there are no 2-chains for the graph X . Thus $H_1(X) = \mathbb{Z} \oplus \mathbb{Z}$ essentially enumerates the number of independent one-dimensional cycles in X . The rank of $H_1(X)$ is known as the *first Betti number*, $B_1(X)$, which is equal to 2 for the graph X .

For a general graph with $|E|$ edges and $|V|$ vertices $H_1 = (\oplus \mathbb{Z})^{|E|-|V|+1}$ and hence $B_1 = |E| - |V| + 1$. From a familiar result in graph theory we identify $|E| - |V| + 1$ to be the number of independent cycles of the graph under consideration.

We can also compute $H_0(X) = \text{Ker}(\partial_0)/\text{Im}(\partial_1)$ for the graph X in Fig. 14. Now $\text{Ker}(\partial_0) = \mathbb{Z} \oplus \mathbb{Z} \oplus \mathbb{Z}$ is generated by x, y, z and $\text{Im}(\partial_1) = \mathbb{Z} \oplus \mathbb{Z} \oplus \mathbb{Z}$ is generated by $y - x, z - y, x - z$. To take the quotient we equate each element in $\text{Im}(\partial_1)$ to 0 which implies $H_0(X) = \mathbb{Z}$. From this example we can convince ourselves that all vertices in a connected component of a general graph will be identified. Thus H_0 for a general graph measures the number of connected components of the graph and denotes the *zeroth Betti number*. Clearly for the graph X in Fig. 14, $B_0(X) = 1$.

References

- [1] C. Nayak, S. H. Simon, A. Stern, M. Freedman, S. D. Sarma, *Non-Abelian Anyons and Topological Quantum Computation*, Rev. Mod. Phys. **80**, 1083 (2008) and [arXiv:0707.1889 [cond-mat.str-el]].
- [2] M. H. Freedman, A. Y. Kitaev, M. J. Larsen, Z. Wang, *Topological Quantum Computation*, Bull. Amer. Math. Soc. **40** (2003), 31-38 and [arXiv:quant-ph/0101025].
- [3] J. K. Pachos, *Introduction to topological quantum computation*, Cambridge Univ. Press, 2012.
- [4] A. Y. Kitaev, *Fault tolerant quantum computation by anyons*, Annals Phys. **303** (2003) 2-30 and [arXiv:quant-ph/9707021 [quant-ph]].
- [5] A. Y. Kitaev, J. Preskill, *Topological entanglement entropy*, Phys. Rev. Lett. **96** (2006) 110404 and [arXiv:hep-th/0510092].
- [6] M. de W. Propitius, F. A. Bais, *Discrete gauge theories*, [arXiv:hep-th/9511201].
- [7] S. Majid, *Foundations of quantum group theory*, Cambridge Univ. Press, 1995.
- [8] O. Buerschaper, J. M. Mombelli, M. Christandl, M. Aguado, *A hierarchy of topological tensor network states*, J. Math. Phys. **54**, 012201 (2013) and [arXiv:1007.5283 [cond-mat.str-el]].

- [9] M. J. B. Ferreira, P. Padmanabhan, P. Teotonio-Sobrinho, *2D Quantum Double Models From a 3D Perspective*, J. Phys. A: Math. Theor. **47** (2014) 375204 (50pp) and [arXiv:1310.8483 [cond-mat.str-el]].
- [10] A. Hatcher, *Algebraic topology*, Cambridge Univ. Press, 2001.
- [11] A.P. Balachandran, E. Ercolessi, *Statistics on networks*, Int. J. Mod. Phys. A Vol. **07**, No. 19, 4633-4654 (1992).
- [12] P. Kuchment, *Quantum graphs: I. Some basic structures*, Waves Random Media **14** (2004) S107-S128.
- [13] P. Kuchment, *Graph models of wave propagation in thin structures*, Waves in Random Media **12** (2002), no. 4, R1-R24.
- [14] T. Inoue, M. Sakamoto, I. Ueba, *Instantons and Berry's connections on quantum graph*, [arXiv:2104.02311 [hep-th]].
- [15] J. Alicea, Y. Oreg, G. Refael, F. von Oppen, M. P. A. Fisher, *Non-Abelian statistics and topological quantum information processing in 1D wire networks*, Nature Physics **7**, 412-417 (2011) and [arXiv:1006.4395 [cond-mat.mes-hall]].
- [16] J. M. Harrison, J. P. Keating, J. M. Robbins, *Quantum statistics on graphs*, Proc. R. Soc. A. **467** (2011) 212-233 and [arXiv:1101.1535 [math-ph]].
- [17] J. M. Harrison, J. P. Keating, J. M. Robbins, A. Sawicki, *n-Particle Quantum Statistics on Graphs*, Commun. Math. Phys. **330**, 1293-1326 (2014).
- [18] T. Maciazek, A. Sawicki, *Non-abelian Quantum Statistics on Graphs*, Commun. Math. Phys. **371**, 921-973 (2019).
- [19] J. M. Leinaas, J. Myrheim, *On the theory of identical particles*, Nuovo Cim. B **37**, 1-23 (1977).
- [20] B. H. An, T. Maciazek, *Geometric presentations of braid groups for particles on a graph*, [arXiv:2006.15256 [math-ph]].
- [21] T. Maciazek, *Non-abelian anyons on graphs from presentations of graph braid groups*, Acta Physica Polonica A, Vol. **136**, No. 5, 824-833 (2019) and [arXiv:1909.02098 [math-ph]].
- [22] D. Farley, L. Sabalka, *Presentations of Graph Braid Groups*, Forum Math. **24** (2012), 827-859 and [arXiv:0907.2730 [math.GR]].
- [23] R. Costa de Almeida, J. P. Ibieta-Jimenez, J. Lorca Espiro, P. Teotonio-Sobrinho, *Topological Order from a Cohomological and Higher Gauge Theory perspective*, [arXiv:1711.04186 [math-ph]].
- [24] J. P. Ibieta-Jimenez, M. Petrucci, L. N. Queiroz Xavier, P. Teotonio-Sobrinho, *Topological Entanglement Entropy in d-dimensions for Abelian Higher Gauge Theories*, JHEP **2020**, 167 (2020) and [arXiv:1907.01608 [cond-mat.str-el]].
- [25] M. J. B. Ferreira, J. P. Ibieta-Jimenez, P. Padmanabhan, P. Teotonio-Sobrinho, *A Recipe for Constructing Frustration-Free Hamiltonians with Gauge and Matter Fields in One and Two Dimensions*, J. Phys. A: Math. Theor. **48** 485206 (2015) and [arXiv:1503.07601 [cond-mat.str-el]].

- [26] A. Bullivant, M. Calcada, Z. Kadar, P. Martin, J. F. Martins, *Topological phases from higher gauge symmetry in 3+1D*, Phys. Rev. B **95**, 155118 (2017) and [arXiv:1606.06639 [cond-mat.str-el]].
- [27] A. Bullivant, M. Calcada, Z. Kadar, J. F. Martins, P. Martin, *Higher lattices, discrete two-dimensional holonomy and topological phases in (3+1) D with higher gauge symmetry*, Reviews in Mathematical Physics, Vol. **32**, No. 04, 2050011 (2020) and [arXiv:1702.00868 [math-ph]].
- [28] J. C. Baez, J. Huerta, *An Invitation to Higher Gauge Theory*, General Relativity and Gravitation **43** (2011), 2335-2392 and [arXiv:1003.4485v2 [hep-th]].
- [29] D. J. A. Welsh, C. Merino, *The Potts model and the Tutte polynomial*, Journal of Mathematical Physics **41**, 1127 (2000).
- [30] Y. Zhang, T. Grover, A. Turner, M. Oshikawa, A. Vishwanath, *Quasi-particle Statistics and Braiding from Ground State Entanglement*, Phys. Rev. B **85**, 235151 (2012) and [arXiv:1111.2342 [cond-mat.str-el]].
- [31] H.-C. Jiang, Z. Wang, L. Balents, *Identifying Topological Order by Entanglement Entropy*, Nature Physics **8**, 902-905 (2012) and [arXiv:1205.4289 [cond-mat.str-el]].
- [32] M. Hamermesh, *Group theory and its applications to physical problems*, Dover Reprint, 2003.
- [33] J. A. Bondy, U. S. R. Murty, *Graph Theory with Applications*, North Holland, 1976.
- [34] M. B. Hastings, *An Area Law for One Dimensional Quantum Systems*, JSTAT, P08024 (2007) and [arXiv:0705.2024 [quant-ph]].
- [35] A. Hamma, R. Ionicioiu, P. Zanardi, *Bipartite entanglement and entropic boundary law in lattice spin systems*, Phys. Rev. A **71**, 022315 (2005) and [arXiv:quant-ph/0409073].
- [36] A. Hamma, R. Ionicioiu, P. Zanardi, *Ground state entanglement and geometric entropy in the Kitaev's model*, Phys. Lett. A **337**, 22 (2005) and [arXiv:quant-ph/0406202].
- [37] D. Fattal, T. S. Cubitt, Y. Yamamoto, S. Bravyi, I. L. Chuang, *Entanglement in the stabilizer formalism*, [arXiv:quant-ph/0406168].
- [38] M. Levin, X.-G. Wen, *Detecting topological order in a ground state wave function*, Phys. Rev. Lett. **96**, 110405 (2006) and [arXiv:cond-mat/0510613 [cond-mat.str-el]].
- [39] M. A. Levin and X. G. Wen, *String net condensation: A Physical mechanism for topological phases*, Phys. Rev. B **71** (2005) 045110 and [arXiv:cond-mat/0404617 [cond-mat]].
- [40] K. Patel, *Theoretical Generalizations of Topological Phases and Topological Entanglement Entropy*, PhD Thesis, <https://escholarship.org/uc/item/77314761>.
- [41] S. D. Geraedts, O. I. Motrunich, *Exact Models for Symmetry-Protected Topological Phases in One Dimension*, [arXiv:1410.1580 [cond-mat.stat-mech]].
- [42] M. H. Freedman and D. A. Meyer, *Projective plane and planar quantum codes*, Found. Comput. Math. **1**, 325-332 (2001) and [arXiv:quant-ph/9810055 [quant-ph]].
- [43] S. B. Bravyi and A. Y. Kitaev, *Quantum codes on a lattice with boundary*, [arXiv:quant-ph/9811052 [quant-ph]].

- [44] D. V. Else, C. Nayak, *Classifying symmetry-protected topological phases through the anomalous action of the symmetry on the edge*, Phys. Rev. B **90**, 235137 (2014) and [arXiv:1409.5436 [cond-mat.str-el]].
- [45] M. Pretko, X. Chen, Y. You, *Fracton Phases of Matter*, Int. J. of Mod. Phy. A Vol. **35**, No. 06, 2030003 (2020) and [arXiv: 2001.01722 [cond-mat.str-el]].
- [46] M.-Y. Li, P. Ye, *Fracton physics of spatially extended excitations*, Phys. Rev. B **101**, 245134 (2020) and [arXiv:1909.02814 [cond-mat.str-el]] .
- [47] M.-Y. Li, P. Ye, *Fracton physics of spatially extended excitations. II. Polynomial ground state degeneracy of exactly solvable models*, [arXiv:2104.05735 [cond-mat.str-el]].
- [48] G. 't Hooft, *A Property of Electric and Magnetic Flux in Nonabelian Gauge Theories*, Nucl. Phys. B **153**, 141-160 (1979).